Pseudo-compressibility, dispersive model and acoustic waves in shallow water flows

Anne-Sophie Bonnet-Ben Dhia, Marie-Odile Bristeau, Edwige Godlewski, Sébastien Imperiale, Anne Mangeney, Jacques Sainte-Marie

Pseudo-compressibility, dispersive model and acoustic waves in shallow water flows

Anne-Sophie Bonnet-Ben Dhia, Marie-Odile Bristeau and Edwige Godlewski and Sébastien Impériale and Anne Mangeney and Jacques Sainte-Marie

Keywords: shallow water flows, dispersive models, compressible models, water and acoustic waves, projection-correction schemes, finite volumes

Math. classification. 65M12; 74S10; 76M12; 35L65; 35Q30; 35Q35; 76D05; 76Q05.

1 Presentation

The non linear shallow water model with topography [6] is widely used to describe geophysical flows and an extensive literature exists for its numerical approximation [17, 19, 9, 2, 5]. But the classical shallow water equations rely on the hydrostatic assumption and many shallow water type models taking into consideration the dispersive effects have been proposed and studied in the literature, see [18, 8, 7, 21, 20, 11, 14, 10, 1], the list being non-exhaustive.

Considering a two-dimensional domain $\Omega \subset \mathbb{R}^2$ delimited by the boundary $\Gamma = \Gamma_{in} \cup \Gamma_{out} \cup \Gamma_s$ as described in Fig. 1-*(a)*, some of the authors have proposed a family

Anne-Sophie Bonnet-Ben Dhia, Inria Saclay, rue Honoré d'Estienne d'Orves F-91120 Palaiseau e-mail: Anne-Sophie.Bonnet-Bendhia@ensta-paris.fr · Marie-Odile Bristeau, Inria Paris, 2 rue Simone Iff, 75589 Paris Cedex 12 and Sorbonne University, univ. Paris-Diderot SPC, CNRS, Laboratoire Jacques-Louis Lions, F-75005 Paris e-mail: Marie-Odile.Bristeau@inria.fr Edwige godlewski, Sorbonne University, univ. Paris-Diderot SPC, CNRS, Laboratoire Jacques-Louis Lions, F-75005 Paris and Inria Paris, 2 rue Simone Iff, 75589 Paris Cedex 12e-mail: Edwige.Godlewski@upmc.fr · Sébastien Impériale, Inria Saclay rue Honoré d'Estienne d'Orves F-91120 Palaiseau and Laboratoire de mécanique des solides, Route de Saclay, F- 91120 Palaiseau e-mail: Sebastien.Imperiale@inria.fr · Anne Mangeney, Inria Paris, 2 rue Simone Iff, 75589 Paris Cedex 12 and Sorbonne université, Univ. Paris-Diderot SPC, CNRS, Laboratoire Jacques-Louis Lions, F-75005 Paris and univ. Paris Diderot, Sorbonne Paris Cité, Institut de Physique du Globe de Paris, Seismology Group, 1 rue Jussieu, Paris F-75005 e-mail: Anne.Mangeney@ipgp.fr · Jacques Sainte-Marie, Inria Paris, 2 rue Simone Iff, 75589 Paris Cedex 12 and Sorbonne Université, univ. Paris-Diderot SPC, CNRS, Laboratoire Jacques-Louis Lions, F-75005 Paris e-mail: Jacques.Sainte-Marie@inria.fr

of 2d shallow water dispersive models written under the form [1]

$$\frac{\partial h}{\partial t} + \frac{\partial (hu)}{\partial x} + \frac{\partial (hv)}{\partial y} = 0, \tag{1}$$

$$\frac{\partial (hu)}{\partial t} + \frac{\partial}{\partial x}\left(hu^2 + \frac{g}{2}h^2 + hp\right) + \frac{\partial (huv)}{\partial y} = -(gh + \frac{\gamma^2}{2}p)\frac{\partial z_b}{\partial x}, \tag{2}$$

$$\frac{\partial (hv)}{\partial t} + \frac{\partial (huv)}{\partial x} + \frac{\partial}{\partial y}\left(hv^2 + \frac{g}{2}h^2 + hp\right) = -(gh + \frac{\gamma^2}{2}p)\frac{\partial z_b}{\partial y}, \tag{3}$$

$$\frac{\partial (hw)}{\partial t} + \frac{\partial (huw)}{\partial x} + \frac{\partial (hvw)}{\partial y} = \gamma p, \tag{4}$$

$$\gamma w = -h\frac{\partial u}{\partial x} + \frac{\gamma^2}{2}u\frac{\partial z_b}{\partial x} - h\frac{\partial v}{\partial y} + \frac{\gamma^2}{2}v\frac{\partial z_b}{\partial y}, \tag{5}$$

where $\mathbf{u}(t, \mathbf{x}) = (u, v, w)^T$ is the velocity of the fluid with $\mathbf{x} = (x, y)$, p is the non-hydrostatic part of the fluid pressure, the total pressure is given by $p_{tot} = gh/2 + p$ and g represents the gravity acceleration. The value of the parameter $\gamma \in \mathbb{R}$ will be discussed in Remark 1. The water depth (resp. the topography profile) is denoted $h(t, \mathbf{x})$ (resp. $z_b(\mathbf{x})$) and the free surface is defined by (see Fig. 1-*(b)*)

$$\eta(t, \mathbf{x}) := h(t, \mathbf{x}) + z_b(\mathbf{x}). \tag{6}$$

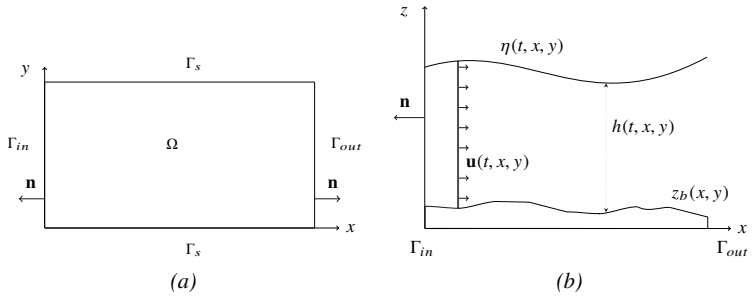

Fig. 1 Model domain and notations, *(a)* view from above and *(b)* vertical cross section.

For smooth solutions, the system (1)-(5) satisfies the following energy balance

$$\frac{\partial E}{\partial t} + \nabla_0 . \Big(\mathbf{u}(E + \frac{g}{2}h^2 + hp)\Big) = 0, \tag{7}$$

with the operator $\nabla_0 = (\frac{\partial}{\partial x}, \frac{\partial}{\partial y}, 0)^T$ and

$$E = h(u^2 + v^2 + w^2)/2 + g(\eta^2 - z_b^2)/2. \tag{8}$$

The system (1)-(5) defines a family $\{\mathcal{M}_\gamma\}$ of dispersive models written in the more compact form

$$\frac{\partial h}{\partial t} + \nabla_0 \cdot (h\mathbf{u}) = 0, \tag{9}$$

$$\frac{\partial (h\mathbf{u})}{\partial t} + \nabla_0 \cdot (h\mathbf{u} \otimes \mathbf{u}) + \nabla_0 (\frac{g}{2} h^2) + \nabla_{sw}^\gamma \, p = -gh\nabla_0 (z_b), \tag{10}$$

$$\mathrm{div}_{sw}^\gamma \, (\mathbf{u}) = 0, \tag{11}$$

where the shallow water versions of the gradient and divergence operators are defined by

$$\nabla_{sw}^\gamma \, f = \begin{pmatrix} h\frac{\partial f}{\partial x} + f\frac{\partial \zeta}{\partial x} \\ h\frac{\partial f}{\partial y} + f\frac{\partial \zeta}{\partial y} \\ -\gamma f \end{pmatrix}, \tag{12}$$

$$\mathrm{div}_{sw}^\gamma \, (\mathbf{w}) = \frac{\partial (hw_1)}{\partial x} + \frac{\partial (hw_2)}{\partial y} - w_1 \frac{\partial \zeta}{\partial x} - w_2 \frac{\partial \zeta}{\partial y} + \gamma w_3, \tag{13}$$

for $\mathbf{w} = (w_1, w_2, w_3)^T$ and

$$\zeta = h + \frac{\gamma^2}{2} z_b. \tag{14}$$

Whereas ζ depends on γ, for the sake of simplicity, we have adopted a simplified notation and ζ_γ is replaced by ζ.

The model studied in this paper consists in a compressible version of the model (9)-(11) where the divergence free constraint (11) is replaced by an evolution equation – a relaxed version of (11) – modeling the propagation of acoustic-type waves.

Remark 1 The value of the parameter γ is discussed in [1]. Here we just recall the two extreme hydraulic regimes that can be represented by shallow water models. First the case where $u \ll \sqrt{gh}$ i.e. the fluid velocity is very small compared to the water wave velocity or equivalently the Froude number is very low. In this situation the value $\gamma = \sqrt{3}$ is well adapted since $\mathcal{M}_{\sqrt{3}}$ corresponds to the well known Green-Naghdi model [18]. Another typical situation is the case of advection dominated flows – u cannot be neglected with respect to $\sqrt{gh}$ – where the value $\gamma = 2$ is more appropriate.

The numerical analysis of the system (9)-(11) is studied in [1] and a numerical scheme based on a projection-correction scheme [12] has been proposed. Since the model (9)-(11) appears as an extension of the classical Saint-Venant system, the hyperbolic part is treated using a finite volume approach – explicit in time – coupled with the resolution of a saddle point problem – implicit in time – corresponding to an elliptic-type equation for the contribution of the dispersive terms.

Because of the divergence free constraint (11) used to approximate the non-hydrostatic part of the pressure p, an implicit treatment is natural (see Sec. 3.2) but it significantly increases the computational costs. Indeed, an explicit in time scheme constrained by a CFL condition is required for the approximation of the

hyperbolic part implying small time steps but simple computations of the numerical fluxes. Whereas the dispersive terms are obtained though the resolution of an elliptic equation for the whole domain. Therefore, for the numerical approximation of the model (9)-(11) over a 2D geometrical domain discretized with N cells, at each time step we have to compute $O(N)$ numerical fluxes and to perform the resolution of a linear symmetric problem. For a stationary linear symmetric problem having at our disposal a good preconditioner, the resolution cost can be estimated as $O(N \log N)$ computations but in our situation, the matrices depend on time – and hence have to be built at each time step – and we do not have any high-performance preconditioner. Hence the computational costs can be estimated as $O(N^{3/2})$, the resolution of the elliptic part becoming very limitative.

In this paper we propose, starting from the compressible Navier-Stokes, a modified version of (9)-(11) allowing to propagate both water and acoustic-type waves. The proposed model consists in modifying Eq. (11) in order to include compressibility effects. The new formulation has another advantage since it is possible to discretize it with a fully explicit time scheme and the computational costs are asymptotically $O(N/\sqrt{\varepsilon})$, $\sqrt{\varepsilon}$ being a parameter that will be precised later. Even if the parameter ε can be small, in 2d cases or with fine meshes we have $\varepsilon N \gg 1$ and hence $O(N/\sqrt{\varepsilon}) \ll O(N^{3/2})$.

This paper is organized as follows. First starting from the 3d compressible Navier-Stokes equations, we derive a 2d shallow water model where the acoustic waves – that can be seen as pseudo-compressibility effects – are considered. Then a numerical scheme – explicit in time – is proposed for this 2d model and its properties are studied. Some stability properties – especially a discrete entropy inequality – for the proposed scheme are established in the 1d context. Finally for a well known test case, an illustration comparing the implicit strategy and the resolution of the pseudo-compressible model are presented and the associated computational costs are given.

2 A compressible and dispersive model in shallow water context

In this section, we derive a shallow water approximation of the 3d compressible Navier-Stokes with free surface. The model obtained in prop. 2 propagates both water and acoustic waves and its dispersive properties are studied. Finally, considering the acoustic velocity is very large compared to the gravity wave velocity, we propose a new formulation as a pseudo-compressible shallow water dispersive model.

2.1 The compressible Navier-Stokes-Fourier system

We consider the classical compressible Navier-Stokes system describing a free surface gravitational 3d flow over a bottom topography $z_b(x, y)$,

$$\frac{\partial \tilde{\rho}}{\partial t} + \nabla \cdot (\tilde{\rho}\mathbf{U}) = 0, \tag{15}$$

$$\frac{\partial (\tilde{\rho}\mathbf{U})}{\partial t} + \nabla \cdot (\tilde{\rho}\mathbf{U} \otimes \mathbf{U}) + \nabla \tilde{p} - \nabla \cdot \sigma = \tilde{\rho}\mathbf{g}, \tag{16}$$

$$\frac{\partial}{\partial t}\left(\tilde{\rho}\frac{|\mathbf{U}|^2}{2} + \tilde{\rho}e\right) + \nabla \cdot \left((\tilde{\rho}\frac{|\mathbf{U}|^2}{2} + \tilde{\rho}e + \tilde{p} - \sigma)\mathbf{U}\right) = -\nabla \cdot Q_{\tilde{T}} - \tilde{\rho}\mathbf{g} \cdot \mathbf{U}, \tag{17}$$

where $\mathbf{U} = (u_1, u_2, u_3)^T$ is the velocity, $\tilde{\rho}$ is the density, $\tilde{p}$ is the fluid pressure, σ is the viscosity stress and $\mathbf{g} = (0, 0, -g)^T$ represents the gravity forces. The internal specific energy is denoted by e, the temperature by $\tilde{T}$. The heat flux $Q_{\tilde{T}}$ obeys the Fourier law $Q_{\tilde{T}} = -\tilde{\lambda}\nabla\tilde{T}$, which explains the name "Navier-Stokes-Fourier", $\tilde{\lambda}$ being the heat conductivity. The symbol ∇ denotes $\nabla = \left(\frac{\partial}{\partial x}, \frac{\partial}{\partial y}, \frac{\partial}{\partial z}\right)^T$. In the following, we will also use the notation $\mathbf{v} = (u_1, u_2)^T$ for the horizontal velocity and $\nabla_{x,y}$ corresponds to the projection of ∇ on the horizontal plane i.e. $\nabla_{x,y} = \left(\frac{\partial}{\partial x}, \frac{\partial}{\partial y}\right)^T$. The square norm of the velocity vector is $|\mathbf{U}|^2 = u_1^2 + u_2^2 + u_3^2$.

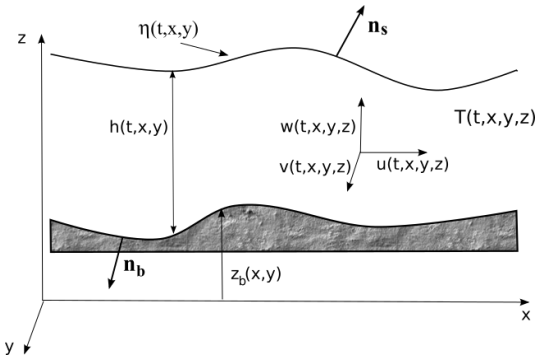

Fig. 2 Flow domain with water height $h(t, \mathbf{x})$, free surface $\eta(t, \mathbf{x})$ and bottom $z_b(\mathbf{x})$.

The term $\tilde{\rho}\mathbf{g}\cdot\mathbf{U} = -\tilde{\rho}gu_3$ in (17) prevents this equation from being directly a local energy conservation law. Nevertheless one can write it in terms of the gravitational potential energy, $\tilde{\rho}gu_3 = \partial_t(\tilde{\rho}gz) + \nabla \cdot (\tilde{\rho}gz\mathbf{U})$, which leads to a conservative equation. The integration of this term is performed below, see Remark 2. For the sake of simplicity we work here with the local energy equation (17).

Regarding constitutive equations, we assume that the fluid is Newtonian i.e. the viscous part of the Cauchy stress depends linearly on the velocity and is given by

$$\sigma = \xi\nabla \cdot \mathbf{U}\mathbf{1} + 2\mu D(\mathbf{U}),$$

where μ is the viscosity coefficient, ξ is the second viscosity and $D(\mathbf{U}) = (\nabla\mathbf{U} + (\nabla\mathbf{U})^T)/2$.

Among the thermodynamic variables $\tilde{\rho}, \tilde{p}, \tilde{T}, e$, only two of them are independent. Indeed, we have a state law under the form

$$f(\tilde{\rho}, \tilde{T}, \tilde{p}) = 0, \tag{18}$$

where f is a real valued function. We give some examples below. Moreover, the thermodynamic variables are linked by the identity

$$de = \frac{\tilde{p}}{\tilde{\rho}^2} d\tilde{\rho} + \tilde{T} ds, \tag{19}$$

where s is the specific entropy of the fluid. Classically, in order to have a convenient entropy dissipation one has to assume that $-s$ is a convex function of $1/\tilde{\rho}, e$.

2.1.1 Boundary conditions at the bottom

Let $\mathbf{n}_b$ and $\mathbf{n}_s$ be the unit outward normals at the bottom and at the free surface respectively, defined by (see Fig 2)

$$\mathbf{n}_b = \frac{1}{\sqrt{1 + |\nabla_{x,y} z_b|^2}} \begin{pmatrix} \nabla_{x,y} z_b \\ -1 \end{pmatrix}, \qquad \mathbf{n}_s = \frac{1}{\sqrt{1 + |\nabla_{x,y} \eta|^2}} \begin{pmatrix} -\nabla_{x,y} \eta \\ 1 \end{pmatrix}.$$

On the bottom we prescribe an impermeability condition

$$\mathbf{U} \cdot \mathbf{n}_b = 0, \tag{20}$$

and a friction condition given e.g. by a Navier law

$$(\Sigma \cdot \mathbf{n}_b) \cdot \mathbf{t}_i = -\kappa \mathbf{U} \cdot \mathbf{t}_i, \quad i = 1, 2, \tag{21}$$

with κ a Navier coefficient and $(\mathbf{t}_i, i = 1, 2)$ two tangential vectors.

2.1.2 Boundary conditions at free surface

On the free surface $z = \eta(t, x, y)$, we use the kinematic boundary condition

$$\frac{\partial \eta}{\partial t} + \mathbf{v}(t, x, y, \eta) \cdot \nabla_{x,y} \eta - u_3(t, x, y, \eta) = 0, \tag{22}$$

and the no stress condition

$$\Sigma \cdot \mathbf{n}_s = -p^a(t, x, y) \mathbf{n}_s + W(t, x, y) \mathbf{t}_s, \tag{23}$$

where $p^a(t, x, y)$, $W(t, x, y)$ are two given external forcings, p^a (resp. W) mimics the effects of the atmospheric pressure (resp. the wind blowing at the free surface) and $\mathbf{t}_s$

is a given unit horizontal vector. Throughout the paper we assume $p^a = cst$, $W = 0$. For the temperature, Neumann or Dirichlet boundary conditions can be considered.

Remark 2 Multiplying the mass conservation (15) by z we get the identity

$$\frac{\partial(z\tilde{\rho})}{\partial t} + \nabla \cdot (z\tilde{\rho}\mathbf{U}) = \tilde{\rho}u_3. \tag{24}$$

Computing the integral along the vertical axis of relation (24) and using the boundary conditions (22),(20) one obtains

$$\frac{\partial}{\partial t}\int_{z_b}^{\eta} gz\tilde{\rho}dz + \nabla_{x,y} \cdot \int_{z_b}^{\eta} gz\tilde{\rho}\mathbf{v}dz = \int_{z_b}^{\eta} g\tilde{\rho}u_3 dz, \tag{25}$$

which is the integrated local conservation of gravitational potential energy.

2.2 Thermodynamic considerations

Taking the scalar product of Eq. (16) by $\mathbf{U}$ yields the kinetic energy equation

$$\frac{\partial}{\partial t}\left(\tilde{\rho}\frac{|\mathbf{U}|^2}{2}\right) + \nabla \cdot \left((\tilde{\rho}\frac{|\mathbf{U}|^2}{2} + \tilde{p} - \sigma)\mathbf{U}\right) = \tilde{p}\nabla \cdot \mathbf{U} - \sigma : D(\mathbf{U}) + \tilde{\rho}\mathbf{g}.\mathbf{U}. \tag{26}$$

Subtracting (26) to (17) gives the equation for the internal energy

$$\frac{\partial(\tilde{\rho}e)}{\partial t} + \nabla \cdot (\tilde{\rho}e\mathbf{U}) = -\tilde{p}\nabla \cdot \mathbf{U} + \sigma : D(\mathbf{U}) - \nabla \cdot Q_{\tilde{T}},$$

or equivalently

$$\tilde{\rho}\frac{De}{Dt} = -\tilde{p}\nabla \cdot \mathbf{U} + \sigma : D(\mathbf{U}) - \nabla \cdot Q_{\tilde{T}}, \tag{27}$$

with the classical notation $D/Dt \equiv \partial/\partial t + \mathbf{U}\cdot\nabla$. We can write the continuity equation (15) as

$$\tilde{\rho}\frac{D\tilde{\rho}}{Dt} + \tilde{\rho}^2\nabla \cdot \mathbf{U} = 0. \tag{28}$$

With the thermodynamic relation (19) one can write $ds = de/\tilde{T} - (\tilde{p}/\tilde{T}\tilde{\rho}^2)d\tilde{\rho}$, thus multiplying (27) by $1/\tilde{T}$ and (28) by $-\tilde{p}/\tilde{T}\tilde{\rho}^2$ we obtain

$$\tilde{\rho}\frac{Ds}{Dt} = \frac{1}{\tilde{T}}\sigma : D(\mathbf{U}) - \frac{1}{\tilde{T}}\nabla \cdot Q_{\tilde{T}}. \tag{29}$$

This can be written also

$$\frac{\partial(\tilde{\rho}s)}{\partial t} + \nabla \cdot (\tilde{\rho}s\mathbf{U}) = \frac{1}{\tilde{T}}\sigma : D(\mathbf{U}) - \nabla \cdot \frac{Q_{\tilde{T}}}{\tilde{T}} - Q_{\tilde{T}} \cdot \frac{\nabla\tilde{T}}{\tilde{T}^2}, \tag{30}$$

which gives the increase with time of $\int \tilde{\rho}s$, the second principle of thermodynamics.

Remark 3 Notice that from Eqs. (28),(29), we also get the equation governing the temperature T

$$\tilde{\rho}\frac{DT}{Dt} + \tilde{\rho}^2\left(\frac{\partial T}{\partial \tilde{\rho}}\right)_s \nabla\cdot\mathbf{U} = \frac{1}{T}\left(\frac{\partial T}{\partial s}\right)_{\tilde{\rho}} (\sigma : D(\mathbf{U}) - \nabla\cdot Q_T)\,. \tag{31}$$

The state law (18) or (19) plays the role of a closure relation. It can have several forms, for example $e = e(\tilde{\rho}, s)$, but in many cases it is easier to specify an equation of state having the form $\tilde{p} = \tilde{p}(\tilde{\rho}, \tilde{T})$ rather than $e = e(\tilde{\rho}, s)$, and this leads to

$$d\tilde{p} = \left(\frac{\partial \tilde{p}}{\partial \tilde{\rho}}\right)_{\tilde{T}} d\tilde{\rho} + \left(\frac{\partial \tilde{p}}{\partial \tilde{T}}\right)_{\tilde{\rho}} d\tilde{T}. \tag{32}$$

Therefore, from Eqs. (32),(29) and using Eqs. (28) we get

$$\tilde{\rho}\frac{D\tilde{p}}{Dt} + \tilde{\rho}^2\left(\left(\frac{\partial \tilde{p}}{\partial \tilde{\rho}}\right)_{\tilde{T}} + \left(\frac{\partial \tilde{p}}{\partial \tilde{T}}\right)_{\tilde{\rho}}\left(\frac{\partial \tilde{T}}{\partial \tilde{\rho}}\right)_s\right)\nabla\cdot\mathbf{U} = \frac{1}{\tilde{T}}\left(\frac{\partial \tilde{p}}{\partial \tilde{T}}\right)_{\tilde{\rho}}\left(\frac{\partial \tilde{T}}{\partial s}\right)_{\tilde{\rho}} (\sigma : D(\mathbf{U}) - \nabla\cdot Q_{\tilde{T}})\,. \tag{33}$$

Using the chain rule this can be written

$$\tilde{\rho}\frac{D\tilde{p}}{Dt} + \tilde{\rho}^2\tilde{c}^2\nabla\cdot\mathbf{U} = \frac{1}{\tilde{T}}\left(\frac{\partial \tilde{p}}{\partial s}\right)_{\tilde{\rho}} (\sigma : D(\mathbf{U}) - \nabla\cdot Q_{\tilde{T}})\,, \tag{34}$$

with the sound speed $\tilde{c}$ given by

$$\tilde{c}^2 = \left(\frac{\partial \tilde{p}}{\partial \tilde{\rho}}\right)_{\tilde{T}} + \left(\frac{\partial \tilde{p}}{\partial \tilde{T}}\right)_{\tilde{\rho}}\left(\frac{\partial \tilde{T}}{\partial \tilde{\rho}}\right)_s = \left(\frac{\partial \tilde{p}}{\partial \tilde{\rho}}\right)_s. \tag{35}$$

Neglecting fluid viscosities i.e. $\mu = \xi = 0$ and $\lambda = 0$, the set of equations (15),(16) and (34) writes

$$\frac{\partial \tilde{\rho}}{\partial t} + \nabla\cdot(\tilde{\rho}\mathbf{U}) = 0, \tag{36}$$

$$\frac{\partial(\tilde{\rho}\mathbf{U})}{\partial t} + \nabla\cdot(\tilde{\rho}\mathbf{U}\otimes\mathbf{U}) + \nabla\tilde{p} = \tilde{\rho}\mathbf{g}, \tag{37}$$

$$\frac{\partial(\tilde{\rho}\tilde{p})}{\partial t} + \nabla\cdot(\tilde{\rho}\mathbf{U}\tilde{p}) + \tilde{\rho}^2\tilde{c}^2\nabla\cdot\mathbf{U} = 0, \tag{38}$$

completed with the boundary conditions (20),(22) and with an abuse of notation

$$\tilde{p}(t, x, y, \eta) = p^a(t, x, y). \tag{39}$$

The system (36)-(38) with the boundary conditions (20),(22) and (39) is a reformulation of the compressible Euler system where the acoustic velocity explicitely appears. For the system (36)-(38), the energy balance

$$\frac{\partial}{\partial t}\left(\tilde{\rho}\frac{|\mathbf{U}|^2}{2}+\tilde{\rho}e\right)+\nabla\cdot\left((\tilde{\rho}\frac{|\mathbf{U}|^2}{2}+\tilde{\rho}e+\tilde{p})\mathbf{U}\right)=-\tilde{\rho}\mathbf{g}\cdot\mathbf{U}, \tag{40}$$

holds.

2.3 Acoustic waves and water waves

The system (36)-(38) – completed with the boundary conditions (20),(22) and (39) – is a compressible model with a free surface and hence acoustic and water waves can propagate.

Let us define $\hat{p}$ by

$$\tilde{p}=p^a+\int_z^\eta \tilde{\rho}g\,dz+\hat{p},$$

with $p^a = cst$ thus $\hat{p}$ denotes the non-gravitational part of the pressure. Then the system (36)-(38) with (20) and (22) also writes

$$\frac{\partial\tilde{\rho}}{\partial t}+\nabla\cdot(\tilde{\rho}\mathbf{U})=0, \tag{41}$$

$$\frac{\partial\mathbf{U}}{\partial t}+(\mathbf{U}\cdot\nabla)\mathbf{U}+\frac{1}{\tilde{\rho}}\nabla\hat{p}+\frac{1}{\tilde{\rho}}\nabla\int_z^\eta\tilde{\rho}g\,dz_1=\mathbf{g}, \tag{42}$$

$$\frac{\partial}{\partial t}\left(\int_z^\eta\tilde{\rho}g\,dz+\hat{p}\right)+\mathbf{U}\cdot\nabla\left(\int_z^\eta\tilde{\rho}g\,dz+\hat{p}\right)+\tilde{\rho}\tilde{c}^2\nabla\cdot\mathbf{U}=0, \tag{43}$$

$$\frac{\partial h}{\partial t}+\mathbf{v}_s\cdot\nabla_{x,y}h=u_{3,s}, \tag{44}$$

where the subscript corresponds to the value of the free surface $z=\eta$.

Assuming a flat bottom and in a two dimensional setting (x,z), the system (41)-(44) has the following compact formulation

$$M\frac{\partial Y}{\partial t}+A_x\frac{\partial Y}{\partial x}+A_z\frac{\partial Y}{\partial z}=S, \tag{45}$$

with

$$Y = \begin{pmatrix} \tilde{\rho} \\ u_1 \\ u_3 \\ \hat{p} \\ h \end{pmatrix}, \quad A_x = \begin{pmatrix} u_1 & \tilde{\rho} & 0 & 0 & 0 \\ \frac{g(h-z)}{\tilde{\rho}} & u_1 & 0 & \frac{1}{\tilde{\rho}} & g \\ 0 & 0 & u_1 & 0 & 0 \\ g(h-z)u_1 & \tilde{\rho}\tilde{c}^2 & 0 & u_1 & g\tilde{\rho}u_1 \\ 0 & 0 & 0 & 0 & u_{1,s} \end{pmatrix},$$

$$A_z = \begin{pmatrix} u_3 & 0 & \tilde{\rho} & 0 & 0 \\ 0 & u_3 & 0 & 0 & 0 \\ 0 & 0 & u_3 & \frac{1}{\tilde{\rho}} & 0 \\ 0 & 0 & \tilde{\rho}\tilde{c}^2 & u_3 & 0 \\ 0 & 0 & 0 & 0 & 0 \end{pmatrix}, \quad M = \begin{pmatrix} 1 & 0 & 0 & 0 & 0 \\ 0 & 1 & 0 & 0 & 0 \\ 0 & 0 & 1 & 0 & 0 \\ g(h-z) & 0 & 0 & 1 & \tilde{\rho}g \\ 0 & 0 & 0 & 0 & 1 \end{pmatrix},$$

and

$$S = \begin{pmatrix} 0 \\ \frac{g}{\tilde{\rho}} \frac{\partial}{\partial x} \int_z^h (\tilde{\rho}(t,x,z) - \tilde{\rho}(t,x,z_1)) dz_1 \\ 0 \\ g \frac{\partial}{\partial t} \int_z^h (\tilde{\rho}(t,x,z) - \tilde{\rho}(t,x,z_1)) dz_1 - g u_1 \frac{\partial}{\partial x} \int_z^h (\tilde{\rho}(t,x,z) - \tilde{\rho}(t,x,z_1)) dz_1 + g\tilde{\rho}u_3 \\ u_{3,s} \end{pmatrix}.$$

Considering we are in a shallow water context, we can further assume

$$\frac{\partial \tilde{\rho}}{\partial z} = \frac{\partial u_1}{\partial z} = 0, \tag{46}$$

then the system (45) reduces to

$$M^{sw} \frac{\partial Y}{\partial t} + A_x^{sw} \frac{\partial Y}{\partial x} + A_z \frac{\partial Y}{\partial z} = B, \tag{47}$$

with

$$A_x^{sw} = \begin{pmatrix} u_1 & \tilde{\rho} & 0 & 0 & 0 \\ \frac{g(h-z)}{\tilde{\rho}} & u_1 & 0 & \frac{1}{\tilde{\rho}} & g \\ 0 & 0 & u_1 & 0 & 0 \\ ghu_1 & \tilde{\rho}(\tilde{c}^2 + gz) & 0 & u_1 & g\tilde{\rho}u_1 \\ 0 & 0 & 0 & 0 & u_1 \end{pmatrix}, \quad M^{sw} = \begin{pmatrix} 1 & 0 & 0 & 0 & 0 \\ 0 & 1 & 0 & 0 & 0 \\ 0 & 0 & 1 & 0 & 0 \\ gh & 0 & 0 & 1 & \tilde{\rho}g \\ 0 & 0 & 0 & 0 & 1 \end{pmatrix}.$$

The eigenvalues of the matrix $aA_x^{sw} + bA_z^{sw}$ for $(a,b) \in \mathbb{R}^2$ cannot be easily computed explicitely but the following result holds.

Proposition 1 *The eigenvalues of the matrix* $(M^{sw})^{-1}(aA_x^{sw} + bA_z^{sw})$ *with* $u_1 = u_3 = 0$*, are given by*

$$0, \pm \frac{1}{2} \sqrt{2C_1 \pm 2\sqrt{C_2 + C_3}}, \tag{48}$$

with

$$C_1 = \tilde{c}^2(a^2+b^2) - b^2gh, \quad C_2 = (a^2+b^2)^2\tilde{c}^4 + b^2g^2(8a^2hz - 4a^2z^2 + b^2h^2),$$
$$C_3 = -2b^2(3a^2+b^2)\tilde{c}^2gh.$$

Remark 4 Notice that the quantities C_2 is non-negative whereas C_3 is non-positive. In the situation where $\tilde{c}^2 \geq gh$ that is encountered in practice, then $C_1 \geq 0, C_2 + C_3 \geq 0$ and $C_1 - \sqrt{C_2 + C_3} \geq 0$ therefore the system has 4 real eigenvalues. But when $\tilde{c}^2 \leq gh$ – corrresponding to a less realistic situation – then complex eigenvalues could appear.

Notice also that we are considering situations where $\tilde{c} \gg 1$ (see Eq. (68) below), hence the eigenvalues defined by (48) satisfy the estimates

$$0, \quad \pm\tilde{c}\sqrt{a^2+b^2} + O\Big(\frac{1}{\tilde{c}}\Big), \quad \pm\sqrt{gh}\frac{ab}{\sqrt{a^2+b^2}} + O\Big(\frac{1}{\tilde{c}^2}\Big). \tag{49}$$

Proof (Proof of prop. 1) The proof relies on simple computations that are not presented here. □

2.4 A shallow water approximation

For free surface flows, the vertical direction plays a particular role since it corresponds to the direction of the gravity. Moreover the fluid domain, in our case, is thin in this direction and the following proposition holds.

Proposition 2 *A shallow water approximation of the compressible Euler system* (36)-(38) *leads to the model*

$$\frac{\partial h}{\partial t} + \nabla_0 \cdot (h\mathbf{u}) = 0, \tag{50}$$
$$\frac{\partial (h\mathbf{u})}{\partial t} + \nabla_0 \cdot (h\mathbf{u}\otimes\mathbf{u}) + \nabla_0(\frac{g}{2}h^2) + \nabla_{sw}^{\gamma} p = -gh\nabla_0(z_b), \tag{51}$$
$$\frac{\partial}{\partial t}(hp + \frac{gh^2}{2}) + \nabla_0.\Big((hp + \frac{gh^2}{2})\mathbf{u}\Big) + c^2 \mathrm{div}_{sw}^{\gamma}(\mathbf{u}) = 0, \tag{52}$$

where c is a constant corresponding to a shallow water approximation of the sound speed.

Notice that, whatever the value of γ, the operators $\mathrm{div}_{sw}^{\gamma}$ and ∇_{sw}^{γ} satisfy the duality relation

$$\int_\Omega \nabla_{sw}^{\gamma}(f)\cdot\mathbf{w}d\mathbf{x} = -\int_\Omega \mathrm{div}_{sw}^{\gamma}(\mathbf{w}) f d\mathbf{x} + \int_\Gamma hf\mathbf{w}\cdot\mathbf{n}ds, \tag{53}$$

where the vector $\mathbf{n} = (n_x, n_y, 0)^T$ is the outward unit normal vector to the boundary Γ, see Fig. 1. In Eq. (53), f and $\mathbf{w}$ belong to suitable function spaces that will be precised later.

Notice also that whereas the model described in prop. 2 and the model (9)-(11) differ, we have kept the same notations for the variables of each model. Notice also that Eq. (52) writes

$$\frac{\partial(hp)}{\partial t} + \nabla_0.(hp\mathbf{u}) - \frac{gh^2}{2}\nabla_0.\mathbf{u} + c^2 \mathrm{div}_{sw}^{\gamma}(\mathbf{u}) = 0.$$

Remark 5 When $c \gg 1$, Eq. (52) implies

$$\mathrm{div}_{sw}^{\gamma}(\mathbf{u}) = O\left(\frac{1}{c^2}\right). \tag{54}$$

Besides, using the definitions (14),(13) and (50), we can easily show that

$$\frac{h}{2}\mathrm{div}_{sw}^{\gamma}(\mathbf{u}) = -\frac{\partial}{\partial t}\left(\frac{\eta^2 - z_b^2}{2}\right) - \nabla_0 \cdot \left(\frac{\eta^2 - z_b^2}{2}\mathbf{u}\right) + \gamma\frac{h}{2}w - (\frac{\gamma^2}{2} - 2)\frac{h}{2}\mathbf{u}\cdot\nabla_0 z_b \tag{55}$$

$$= -\frac{\partial}{\partial t}\left(\frac{h\zeta}{2}\right) - \nabla_0 \cdot \left(\frac{h\zeta}{2}\mathbf{u}\right) + \gamma\frac{h}{2}w. \tag{56}$$

Multiplying Eq. (52) by $p + gh/2$ and after simple computations, we obtain the relation

$$\frac{\partial}{\partial t}\left(\frac{h}{2c^2}(p + \frac{gh}{2})^2\right) + \nabla_0.\left(\frac{h}{2c^2}\Big((p + \frac{gh}{2})^2\mathbf{u}\Big)\right) = -(p + \frac{gh}{2})\mathrm{div}_{sw}^{\gamma}(\mathbf{u}), \tag{57}$$

that is – when the density is kept constant and neglecting the viscous and diffusivity terms – the shallow water version of Eq. (27). Hence $e_{sw} = (p + gh/2)^2/(2c^2)$ can be seen as the shallow water version of the internal energy e governed by (27).

Then the following proposition holds.

Proposition 3 *Smooth solutions of the system* (50)-(52) *satisfy the energy balance*

$$\frac{\partial}{\partial t}\Big(\frac{h}{2}|\mathbf{u}|^2 + \frac{h}{2c^2}(p + \frac{gh}{2})^2 + g\left(2 - \frac{\gamma^2}{2}\right)hz_b\Big) + \nabla_0.\Big(\mathbf{u}(\frac{h}{2}|\mathbf{u}|^2 + \frac{h}{2c^2}(p + \frac{gh}{2})^2 + \frac{g}{2}h^2 + g\left(2 - \frac{\gamma^2}{2}\right)hz_b + hp)\Big) = \frac{\gamma h}{2}\mathbf{g}.\mathbf{u}, \tag{58}$$

that is a shallow water version of Eq. (40)*.*

Remark 6 When $c \gg 1$, using (54) and (56), relation (58) leads to

$$\frac{\partial}{\partial t}\Big(\frac{h}{2}|\mathbf{u}|^2+\frac{h}{2c^2}(p+\frac{gh}{2})^2+g\frac{h\zeta}{2}+g\left(2-\frac{\gamma^2}{2}\right)hz_b\Big)+\nabla_0.\Big(\mathbf{u}(\frac{h}{2}|\mathbf{u}|^2 + \frac{h}{2c^2}(p+\frac{gh}{2})^2+\frac{g}{2}h^2+g\frac{h\zeta}{2}+g\left(2-\frac{\gamma^2}{2}\right)hz_b+hp)\Big)=O\left(\frac{1}{c^2}\right). \quad (59)$$

Proof (Proof of prop. 2) It is easy to see (cf. [16, Lemma 2.1]) that a depth averaging of the compressible Euler system with gravity and free surface (36)-(38) completed with the boundary conditions (20),(22),(39) leads to

$$\frac{\partial}{\partial t}\int_{z_b}^{\eta}\tilde{\rho}dz+\nabla_{x,y}.\int_{z_b}^{\eta}\tilde{\rho}\mathbf{v}dz=0, \quad (60)$$

$$\frac{\partial}{\partial t}\int_{z_b}^{\eta}\tilde{\rho}\mathbf{v}dz+\nabla_{x,y}.\int_{z_b}^{\eta}\tilde{\rho}\mathbf{v}\otimes\mathbf{v}dz+\nabla_{x,y}\int_{z_b}^{\eta}\tilde{p}dz=\tilde{p}(t,\mathbf{x},z_b(\mathbf{x}))\nabla_{x,y}z_b, \quad (61)$$

$$\frac{\partial}{\partial t}\int_{z_b}^{\eta}\tilde{\rho}u_3dz+\nabla_{x,y}.\int_{z_b}^{\eta}\tilde{\rho}u_3\mathbf{v}dz=\tilde{p}(t,\mathbf{x},z_b(\mathbf{x}))-\int_{z_b}^{\eta}\tilde{\rho}gdz, \quad (62)$$

$$\frac{\partial}{\partial t}\int_{z_b}^{\eta}\tilde{\rho}\tilde{p}dz+\nabla_{x,y}.\int_{z_b}^{\eta}\tilde{\rho}\tilde{p}\mathbf{v}dz+\int_{z_b}^{\eta}\tilde{\rho}^2\tilde{c}^2\nabla\cdot\mathbf{U}dz=0. \quad (63)$$

As in [1] we are now going to make some assumptions concerning the variations along the vertical axis of the velocity field $\mathbf{U}$, the density $\tilde{\rho}$ and of the pressure $\tilde{p}$. In order to be consistent with the shallow water assumption, the choice

$$u_1(t,\mathbf{x},z)=u(t,\mathbf{x}),\quad u_2(t,\mathbf{x},z)=v(t,\mathbf{x}),\quad \tilde{\rho}(t,\mathbf{x},z)=\rho(t,\mathbf{x}), \quad (64)$$

is natural since it consists in assimilating the horizontal velocity field with its vertical mean. For the velocity u_3 and the pressure $\tilde{p}$, we choose

$$u_3(t,\mathbf{x},z)=\varphi_\delta\left(\frac{\eta-z}{h}\right)w(t,\mathbf{x}), \quad (65)$$

$$\tilde{p}(t,\mathbf{x},z)=p^a+\int_z^{\eta}\tilde{\rho}gdz+\psi_\delta\left(\frac{\eta-z}{h}\right)P(t,\mathbf{x}), \quad (66)$$

where $p^a=cst$ and the two families of functions $\psi_\delta=\psi_\delta(z)$ and $\varphi_\delta=\varphi_\delta(z)$ satisfy

$$\begin{cases}\int_0^1\psi_\delta(z)dz=\int_0^1\varphi_\delta(z)dz=1,\\ \psi_\delta(1)=\delta,\ \psi_\delta(0)=0,\ \varphi_\delta(0)=\delta,\ \varphi_\delta(1)=2.\end{cases} \quad (67)$$

Concerning the expression of $\tilde{c}$, we follow the equation proposed in [15, Eq. (3)]

$$\tilde{c}=\tilde{c}_0(\tilde{T})+a_1(\tilde{T})p+a_2(\tilde{T})p^2,$$

with $\tilde{c}_0(\tilde{T})=1402.3+5.035(\tilde{T}-273.15)$, $a_1(\tilde{T})=1.084\ 10^{-7}+3.378\ 10^{-12}(\tilde{T}-273.15)$, and $a_2(\tilde{T})=7.69410^{-18}-5.08\ 10^{-19}(\tilde{T}-273.15)$, the pressure p being expressed in Pa. Because of the values of $\tilde{c}_0(\tilde{T})$, $a_1(\tilde{T})$ and $a_2(\tilde{T})$ we can assume

$$\tilde{c}\approx\tilde{c}_0(\tilde{T}=293)=c=1502.2\ \mathrm{m.s}^{-1}. \quad (68)$$

Using (64),(65) and (67), we have for the last term in Eq. (63)

$$\int_{z_b}^{\eta} \tilde{\rho}^2\tilde{c}^2\nabla\cdot\mathbf{U}dz = \rho^2c^2\int_{z_b}^{\eta}\nabla\cdot\mathbf{U}dz = \rho^2c^2\left(\varphi_\delta(1)w + h\nabla_0\cdot\mathbf{u} - \varphi_\delta(0)w\right)$$
$$= \rho^2c^2\left(2w + h\nabla_0\cdot\mathbf{u} - \delta\mathbf{u}\cdot\nabla_0 z_b\right),$$

where the boundary condition (20) has been used. Therefore, with the choices (64),(65),(66),(67) and the approximation (68), the system (60)-(63) writes

$$\frac{\partial(\rho h)}{\partial t} + \nabla_0.(\rho h\mathbf{u}) = 0, \tag{69}$$
$$\frac{\partial(\rho hu)}{\partial t} + \frac{\partial}{\partial x}\left(\rho hu^2 + \frac{\rho g}{2}h^2 + hP\right) + \frac{\partial(\rho huv)}{\partial y} = -(\rho gh + \delta P)\frac{\partial z_b}{\partial x}, \tag{70}$$
$$\frac{\partial(\rho hv)}{\partial t} + \frac{\partial(\rho huv)}{\partial x} + \frac{\partial}{\partial y}\left(\rho hv^2 + \frac{\rho g}{2}h^2 + hP\right) = -(\rho gh + \delta P)\frac{\partial z_b}{\partial y}, \tag{71}$$
$$\frac{\partial(\rho hw)}{\partial t} + \nabla_0.(\rho hw\mathbf{u}) = \delta P, \tag{72}$$
$$\frac{\partial}{\partial t}\left(\rho hP + \frac{\rho^2gh^2}{2}\right) + \nabla_0.\left((\rho hP + \frac{\rho^2gh^2}{2})\mathbf{u}\right)$$
$$+\rho^2c^2\left(2w + h\nabla_0\cdot\mathbf{u} - \delta\mathbf{u}\cdot\nabla_0 z_b\right) = 0, \tag{73}$$

where for the sake of simplicity we have considered $p^a = cst$. Furthermore, we assume $\rho = \rho_0 = cst$ in Eqs (69)-(73) and we denote $p = P/\rho_0$. Then a simple change of variables, namely $w = \gamma\hat{w}/2$ with $\gamma^2 = 2\delta$ in the system (69)-(73) leads to the model (50)-(52) where the symbol ˆhas been dropped. □

Proof (Proof of prop. 3) Taking the scalar product of Eq. (51) by $\mathbf{u}$ gives

$$\frac{\partial}{\partial t}\left(\frac{h}{2}|\mathbf{u}|^2\right) + \nabla_0.\left(\mathbf{u}(\frac{h}{2}|\mathbf{u}|^2 + \frac{g}{2}h^2)\right) + \nabla_{sw}^{\gamma}\, p.\mathbf{u} - \frac{g}{2}h^2\nabla_0.\mathbf{u} + gh\nabla_0 z_b.\mathbf{u} = 0. \tag{74}$$

Using the duality relation (53) in (74) and adding the difference between relations (55) and (56) gives (58). □

2.5 The boundary conditions

The set of equations (50)-(52) is completed with the following boundary conditions. We are considering a channel with an inlet Γ_{in} and an outlet Γ_{out} and we impose specific conditions on each of them, see Fig. 1. The inflow is imposed by a given discharge $\mathbf{q}_g$ on Γ_{in}, and a water depth h_g is imposed on Γ_{out}. Finally, we prescribe slip boundary conditions for the velocity at the walls of the channel Γ_s. Hence we have

$$h\mathbf{u}(t,\mathbf{x}) = \mathbf{q}_g(t,\mathbf{x}), \quad \text{on } \Gamma_{in}, \tag{75}$$

$$h(t,\mathbf{x}) = h_g(t,\mathbf{x}), \quad \text{on } \Gamma_{out}, \tag{76}$$

$$\mathbf{u}(t,\mathbf{x}) \cdot \mathbf{n} = 0, \quad \text{on } \Gamma_s. \tag{77}$$

Notice that we can replace the prescribed water depth at the outflow by a free outflow consisting in imposing a Neumann boundary condition over the elevation

$$\nabla_0 h \cdot \mathbf{n} = 0, \quad \text{on } \Gamma_{out}.$$

2.6 Dispersion relation

The model (50)-(52) is a shallow water type model with compressible effects coming from the acoustic wave propagation. A fundamental question is to know what are the velocities of the waves propagating in such a model and typically the influence of the sound speed c over these velocites.

Let us consider the system (50)-(52) in the one-dimensional case and with flat topography. It has the form of an advection-reaction system, namely

$$\frac{\partial Y}{\partial t} + A\frac{\partial Y}{\partial x} + BY = 0, \tag{78}$$

with

$$Y = \begin{pmatrix} h \\ u \\ w \\ p \end{pmatrix}, \quad A = \begin{pmatrix} u & h & 0 & 0 \\ g + \frac{p}{h} & u & 0 & 1 \\ 0 & 0 & u & 0 \\ 0 & c^2 - \frac{gh}{2} & 0 & u \end{pmatrix}, \quad B = \begin{pmatrix} 0 & 0 & 0 & 0 \\ 0 & 0 & 0 & 0 \\ 0 & 0 & 0 & -\frac{\gamma}{h} \\ 0 & 0 & \frac{\gamma c^2}{h} & 0 \end{pmatrix}.$$

Let us introduce $Y_0 \in \mathbb{R}^4$ and k,ω two constants. A necessary condition so that the system (78) admits a solution having the form $Y = Y_0 e^{i(kx-\omega t)}$ is that

$$\det(i\omega I_4 - ikA + B) = 0,$$

I_4 being the identity matrix of dimension 4. This leads to the four roots

$$\frac{\omega}{k} = u \pm \frac{\sqrt{2}}{2}\sqrt{C_{sw,1} \pm \sqrt{(C_{sw,1})^2 - C_{sw,3}}}, \tag{79}$$

with $C_{sw,1} = c^2 + gh + p + c^2\frac{\gamma^2}{(hk)^2}$ and $C_{sw,2} = 4c^2\gamma^2(gh+p)$. As in (49), we can assume that $c \gg 1$ leading to the four approximated roots

$$u \pm \gamma\sqrt{\frac{gh+p}{\gamma^2 - (hk)^2}} + O\left(\frac{1}{c^2}\right), u \pm c\sqrt{1 + \frac{\gamma^2}{(hk)^2}} + O\left(\frac{1}{c}\right). \tag{80}$$

Remark 7 From the estimates (80), it appears that the model (50)-(52) is able to propagate both water waves and acoustic waves. But since we are in a shallow water context, we have $hk \ll 1$ and for the acoustic waves we do not exactly recover the expected velocities $u \pm c$.

2.7 A pseudo-compressible model

As we have seen in the previous paragraph, if c is chosen corresponding to the sound speed in water, then the model (50)-(52) is able to propagate, in a shallow water context, both water and acoustic waves. But since $c \gg 1$, we introduce

$$\varepsilon = \frac{1}{c^2},$$

then the model (50)-(52) can be seen as a pseudo-compressible version of the model (9)-(11) allowing to derive an explicit in time numerical scheme that will be studied in the following section. More precisely Eq. (52) writes

$$\varepsilon \left(\frac{\partial}{\partial t}(hp + \frac{gh^2}{2}) + \nabla_0 . \Big((hp + \frac{gh^2}{2})\mathbf{u} \Big) \right) + \mathrm{div}_{sw}^{\gamma}(\mathbf{u}) = 0,$$

and corresponds to Eq. (11) when ε goes to 0. Following the results obtained in Prop. 3, it is important to notice that in the formulation (50)-(52), the limit $\varepsilon \to 0$ is not singular. Unlike the incompressible limit of compressible models, the limit when $\varepsilon \to 0$ of the model (50)-(52) is the model (9)-(11).

Hence the model (50)-(52) can be seen as

- a dispersive shallow water type model propagating water and acoustic waves,
- a pseudo-compressible dispersive model whose numerical resolution is easier to implement compared to a fully compressible model. This second aspect is studied in the two next sections.

3 The numerical scheme (explicit in time)

In this section, we propose and study a numerical scheme for the system (50)-(52) with $\varepsilon = 1/c^2$. Let us introduce the notations

$$X = \begin{pmatrix} h \\ hu \\ hv \\ hw \end{pmatrix}, \qquad F(X) = \begin{pmatrix} hu & hv \\ hu^2 + \frac{g}{2}h^2 & huv \\ huv & hv^2 + \frac{g}{2}h^2 \\ huw & hvw \end{pmatrix},$$

and $S(X) = (0, -gh\nabla_0(z_b))^T$, $R = (0, \nabla_{sw}^{\gamma} p)^T$ where $\nabla_{sw}^{\gamma} p$ is defined by (12). Then, the system (50)-(52) can be written under the form

$$\frac{\partial X}{\partial t} + \nabla_{x,y} \cdot F(X) + R = S(X), \tag{81}$$

$$\varepsilon\Big(\frac{\partial}{\partial t}(hp + \frac{gh^2}{2}) + \nabla_0.\Big((hp + \frac{gh^2}{2})\mathbf{u}\Big)\Big) + \mathrm{div}_{sw}^{\gamma}(\mathbf{u}) = 0. \tag{82}$$

3.1 Time discretisation

Let us sketch the main steps of the procedure. We set t^0 the initial time and $t^{n+1} = t^n + \Delta t^n$ where Δt^n satisfies a stability condition (CFL) precised later – at the fully discrete level – and the state X^n denotes an approximation of $X(t^n)$. For each time step, we consider an intermediate state which will be denoted with the superscript $^{n+1/2}$. The first step consists in solving the Saint-Venant part of the system (81) with the topography source term and completed with the hyperbolic part of (82) in order to obtain the state $X^{n+1/2} = (h^{n+1/2}, (h\mathbf{u})^{n+1/2})^T$ and $(hp)^{n+1/2}$. Then the state X^{n+1} is computed taking into account the contribution of the non-hydrostatic pressure terms.

More precisely, in the system (81),(82) water waves generally propagate at a lower velocity than acoustic waves. Therefore, we propose an explicit time scheme – constrained by the associated CFL condition – for the Saint-Venant part of Eq. (81). For the dispersive terms, we adopt an iterative resolution scheme explicit in time and constrained by a generally more restrictive CFL condition associated with the sound speed. Hence , the proposed semi-discretization in time consists in the following time-splitting strategy

$$\begin{cases} X^{n+1/2} = X^n - \Delta t^n \nabla_{x,y} \cdot F(X^n) + \Delta t^n S(X^n), \\ (hp)^{n+1/2} = (hp)^n - \frac{g}{2}\Big(h^{n+1/2})^2 - h^n)^2\Big) - \Delta t^n \nabla_0 \cdot \Big(h^n(p^n + \frac{g}{2}(h^n)^2)\mathbf{u}^n\Big), \end{cases} \tag{83}$$

$$\begin{cases} p^{n+1/2,k+1} = p^{n+1/2,k} - \frac{\Delta t^n}{\varepsilon K h^{n+1}} \mathrm{div}_{sw}^{\gamma} \mathbf{u}^{n+1/2,k}, \\ \mathbf{u}^{n+1/2,k+1} = \mathbf{u}^{n+1/2,k} - \frac{\Delta t^n}{K h^{n+1}} \nabla_{sw}^{\gamma} p^{n+1/2,k+1}, \end{cases} \quad k = 1, \ldots, K \tag{84}$$

with $p^{n+1/2,1} = p^{n+1/2}$, $\mathbf{u}^{n+1/2,1} = \mathbf{u}^{n+1/2}$, $p^{n+1} = p^{n+1/2,K+1}$, $\mathbf{u}^{n+1} = \mathbf{u}^{n+1/2,K+1}$ and where for the first component of R we have $h^{n+1} = h^{n+1/2}$ since the first component of X is zero. Notice that the two operators $\mathrm{div}_{sw}^{\gamma}$ and ∇_{sw}^{γ} are defined by Eqs. (12),(13) using h^{n+1}. K is an integer that is defined so that a stability condition, precised later, is satisfied.

3.2 Influence of the pseudo-compressibility over the computational costs

In [1], the authors have studied the model (1)-(5) – that is exactly the model (50)-(52) with $\varepsilon = 0$ – and proposed the following semi-discretization in time

$$X^{n+1/2} = X^n - \Delta t^n \nabla_{x,y} \cdot F(X^n) + \Delta t^n S(X^n), \tag{85}$$

$$(h\mathbf{u})^{n+1} = (h\mathbf{u})^{n+1/2} - \Delta t^n \nabla_{sw}^{\gamma}\, p^{n+1}, \tag{86}$$

$$\mathrm{div}_{sw}^{\gamma}\, \mathbf{u}^{n+1} = 0, \tag{87}$$

in which Eq. (86) allows to correct the predicted value $X^{n+1/2}$ in order to obtain a state which satisfies the divergence free condition (87). The equation satisfied by the pressure is then an elliptic equation which is obtained by applying the shallow water divergence operator $\mathrm{div}_{sw}^{\gamma}$ to Eq. (86) and reads

$$\mathrm{div}_{sw}^{\gamma}\, \left(\frac{1}{h^{n+1}} \nabla_{sw}^{\gamma}\, p^{n+1} \right) = \frac{1}{\Delta t^n} \mathrm{div}_{sw}^{\gamma}\, \left(\frac{(h\mathbf{u})^{n+1/2}}{h^{n+1}} \right). \tag{88}$$

Once the pressure has been determined by the elliptic equation (88), the correction step (86) gives the final step X^{n+1}.

The main drawback of the time scheme (85)-(87) is the numerical cost of the resolution of Eq. (88). And Eq. (52) can be seen as a relaxed version of Eq. (87) allowing to replace the step (86)-(87) by the iterative method (84) applied to the model (81)-(82). More precisely, inserting the second equation of (84) (at iteration $k-1$) into the first one gives the relation

$$\begin{aligned} p^{k+1} &= p^k - \frac{\Delta t^n}{\varepsilon K} \mathrm{div}_{sw}^{\gamma}\, \mathbf{u}^{n+1/2,k-1} + \frac{(\Delta t^n)^2}{\varepsilon K^2 h^{n+1}} \mathrm{div}_{sw}^{\gamma}\, \Big(\frac{1}{h^{n+1}} \nabla_{sw}^{\gamma}\, p^k \Big), \\ &= 2p^k - p^{k-1} + \frac{(\Delta t^n)^2}{\varepsilon K^2 h^{n+1}} \mathrm{div}_{sw}^{\gamma}\, \Big(\frac{1}{h^{n+1}} \nabla_{sw}^{\gamma}\, p^k \Big), \end{aligned} \tag{89}$$

where the superscripts $^{n+1/2}$ have been dropped. Equation (89) appears as an explicit in time discretization of a wave equation. As expected, when ε tends to 0, Eq. (89) reduces to Eq. (88). Likewise, inserting the first equation of (84) into the second one gives the relation

$$\mathbf{u}^{k+1} = 2\mathbf{u}^k - \mathbf{u}^{k-1} + \frac{(\Delta t^n)^2}{\varepsilon K^2 h^{n+1}} \nabla_{sw}^{\gamma}\, \Big(\frac{1}{h^{n+1}} \mathrm{div}_{sw}^{\gamma}\, \mathbf{u}^k \Big). \tag{90}$$

The stability of the two discretizations (89),(90) will be examined in paragraph 4.3.

As already mentioned, if N is the number of cells in the considered mesh, the computational cost of the resolution of (88) is $O(N^{3/2})$ whereas the resolution of (84) is $O(KN) = O(N/\sqrt{\varepsilon})$. And hence, an estimation of ε is required to compare the costs of the explicit and implicit resolutions.

3.3 Choice of ε

If one is interested in the simulation of both water and acoustic waves, ε is chosen so that $\varepsilon = 1/c^2$, c being the sound speed. But if the objective is to approximate a relaxed version of the system (1)-(5) then ε is no more a physical parameter and has to be chosen so that the system (50)-(52) is a good approximation of the system (9)-(11). Hence, at each time step, ε can be chosen according to the computed values of the velocities and of the water depth.

And we can proceed as follows.

When $\varepsilon \ll 1$, using (59), the energy of the model (50)-(52) behaves as

$$h\frac{u^2+v^2+w^2}{2} + \frac{g}{2}h\zeta + g\left(2-\frac{\gamma^2}{2}\right)hz_b + \frac{\varepsilon h}{2}\Big(p+\frac{g}{2}h\Big)^2.$$

Hence, we have to choose ε such that

$$\varepsilon\Big(p+\frac{g}{2}h\Big)^2 \ll u^2+v^2+w^2+g(\eta+z_b)+g\left(4-\gamma^2\right)z_b. \tag{91}$$

Another possibility is to recall that ε is related to the sound speed with $\varepsilon = 1/c^2$ and hence ε has to satisfy

$$\frac{1}{\sqrt{\varepsilon}} = c \gg |u| + |v| + \sqrt{gh},$$

i.e.

$$\varepsilon \ll \frac{1}{(|u|+|v|+\sqrt{gh})^2}. \tag{92}$$

The two conditions (91) and (92) are easy to implement and similar when $|u| + |v| + |w| \ll \sqrt{gh}$. But, in the context of dispersive flows (91) is more appropriate since the vertical velocity w is taken into account.

4 Detailed numerical scheme in 1d

A numerical scheme for the model (9)-(11) has been proposed and studied in [1]. Here we focus on the one dimensional case in order to prove the capability of the pseudo-compressible formulation.

In the one dimensional case, the model (50)-(52) writes

$$\frac{\partial h}{\partial t}+\frac{\partial (hu)}{\partial x}=0, \tag{93}$$

$$\frac{\partial (hu)}{\partial t}+\frac{\partial}{\partial x}\left(hu^2+\frac{g}{2}h^2+hp\right)=-(gh+\frac{\gamma^2}{2}p)\frac{\partial z_b}{\partial x}, \tag{94}$$

$$\frac{\partial (hw)}{\partial t}+\frac{\partial (huw)}{\partial x}=\gamma p, \tag{95}$$

$$\varepsilon\left(\frac{\partial}{\partial t}(hp+\frac{gh^2}{2})+\frac{\partial}{\partial x}\Big((hp+\frac{gh^2}{2})u\Big)\right)+\gamma w+h\frac{\partial u}{\partial x}-\frac{\gamma^2}{2}u\frac{\partial z_b}{\partial x}=0, \tag{96}$$

and the smooth solutions of Eqs. (93)-(96) satisfy the energy equality

$$\begin{aligned}\frac{\partial}{\partial t}\Big(\frac{h}{2}(u^2+w^2)+g\left(2-\frac{\gamma^2}{2}\right)hz_b+\frac{\varepsilon h}{2}(p+\frac{gh}{2})^2\Big)+\frac{\partial}{\partial x}\Big(u(\frac{h}{2}(u^2+w^2)\\ +g\left(2-\frac{\gamma^2}{2}\right)hz_b+\frac{\varepsilon h}{2}(p+\frac{gh}{2})^2+\frac{g}{2}h^2+hp)\Big)=\frac{\gamma gh}{2}w,\end{aligned} \tag{97}$$

or equivalently

$$\frac{\partial}{\partial t}\Big(\bar{E}+\frac{\varepsilon h}{2}(p+\frac{gh}{2})^2\Big)+\frac{\partial}{\partial x}\Big(u(\bar{E}+\frac{\varepsilon h}{2}(p+\frac{gh}{2})^2+\frac{g}{2}h^2+hp)\Big)=O\left(\frac{1}{c^2}\right), \tag{98}$$

with $\bar{E}=h(u^2+w^2)/2+g(\eta^2-z_b^2)/2$, see Prop. 3.

In a more compact form and with obvious notations, the system (93)-(96) becomes

$$\frac{\partial X}{\partial t}+\frac{\partial F(X)}{\partial x}+R=S(X), \tag{99}$$

$$\varepsilon\Big(\frac{\partial (h\hat{p})}{\partial t}+\frac{\partial (hu\hat{p})}{\partial x}\Big)+\mathrm{div}_{sw}^{\gamma}\,(\mathbf{u})=0, \tag{100}$$

with $\mathbf{u}=(u,w)^T$, $\hat{p}=p+gh/2$ and

$$X=\begin{pmatrix}h\\ h\mathbf{u}\end{pmatrix}, \tag{101}$$

$$\nabla_{sw}^{\gamma}f=\begin{pmatrix}h\frac{\partial f}{\partial x}+\frac{\partial \zeta}{\partial x}f\\ -\gamma f\end{pmatrix},\quad \mathrm{div}_{sw}^{\gamma}\,\mathbf{u}=\frac{\partial (hu)}{\partial x}-u\frac{\partial \zeta}{\partial x}+\gamma w. \tag{102}$$

Notice that the fundamental duality relation

$$\int_I p\,\mathrm{div}_{sw}^{\gamma}\,\mathbf{u}\,dx=[hup]_{\partial I}-\int_I \nabla_{sw}^{\gamma}\,p\cdot\mathbf{u}\,dx, \tag{103}$$

holds for any interval I.

4.1 Semi-discrete (in time) scheme

The 1d version of the time discretization (83)-(84) writes

$$\begin{cases} X^{n+1/2} = X^n - \Delta t^n \frac{\partial F(X^n)}{\partial x} + \Delta t^n S(X^n) \\ (h\hat{p})^{n+1/2} = (h\hat{p})^n - \Delta t^n \frac{\partial (h^n \hat{p}^n u^n)}{\partial x} \end{cases} \tag{104}$$

$$\begin{cases} p^{n+1/2,k+1} = p^{n+1/2,k} - \frac{\Delta t^n}{\varepsilon K h^{n+1}} \mathrm{div}_{sw}^{\gamma} \mathbf{u}^{n+1/2,k} \\ \mathbf{u}^{n+1/2,k+1} = \mathbf{u}^{n+1/2,k} - \frac{\Delta t^n}{K h^{n+1}} \nabla_{sw}^{\gamma} p^{n+1/2,k+1} \end{cases} \tag{105}$$

with $p^{n+1/2,1} = p^{n+1/2}$, $\mathbf{u}^{n+1/2,1} = \mathbf{u}^{n+1/2}$ and $p^{n+1} = p^{n+1/2,K+1}$, $\mathbf{u}^{n+1} = \mathbf{u}^{n+1/2,K+1}$ where for the first component of X we have $h^{n+1} = h^{n+1/2}$.

The scheme (104)-(105) is explicit in time so it is important to examine its stability w.r.t. the discretisation step Δt^n, this will be done in paragraph 4.3.

4.2 The semi-discrete (in space) scheme

To approximate the solution $X = (h, hu, hw)^T$, hp of the system (93)-(96), we use a combined finite volume/finite difference framework. We assume that the computational domain is discretized with I nodes x_i, $i = 1, \ldots, I$. We denote C_i the cell $(x_{i-1/2}, x_{i+1/2})$ of length $\Delta x_i = x_{i+1/2} - x_{i-1/2}$ with $x_{i+1/2} = (x_i + x_{i+1})/2$. We denote $X_i = (h_i, q_{x,i}, q_{z,i})^T$ with

$$X_i \approx \frac{1}{\Delta x_i} \int_{C_i} X(t,x)dx,$$

the approximate solution at time t on the cell C_i with $q_{x,i} = h_i u_i$, $q_{z,i} = h_i w_i$. Likewise, for the topography, we define

$$z_{b,i} = \frac{1}{\Delta x_i} \int_{C_i} z_b(x)dx.$$

The non-hydrostatic part of the pressure is discretized on a staggered grid

$$p_{i+1/2} \approx \frac{1}{\Delta x_{i+1/2}} \int_{x_i}^{x_{i+1}} p(t,x)dx,$$

with $\Delta x_{i+1/2} = x_{i+1} - x_i$ and we set $\hat{p}_{i+1/2} = p_{i+1/2} + g h_{i+1/2}/2$ where $h_{i+1/2}$ is defined by $\Delta x_{i+1/2} h_{i+1/2} = (\Delta x_i h_i + \Delta x_{i+1} h_{i+1})/2$.

Now we propose and study the semi-discrete (in space) scheme approximating the model (99)-(100). The semi-discrete scheme writes

$$\Delta x_i \frac{\partial X_i}{\partial t} + (F_{i+1/2-} - F_{i-1/2+}) + R_i = 0, \tag{106}$$

$$\Delta x_{i+1/2} \varepsilon \frac{\partial}{\partial t}\left(h_{i+1/2}\hat{p}_{i+1/2}\right) + \varepsilon\left(F_{\hat{p},i+1} - F_{\hat{p},i}\right) + \mathrm{div}^{\gamma}_{sw,i+1/2}\left(\{\mathbf{u}_j\}\right) = 0, \tag{107}$$

with the numerical fluxes

$$F_{i+1/2+} = \mathcal{F}(X_i, X_{i+1}, z_{b,i}, z_{b,i+1}) + \mathcal{S}_{i+1/2+} \tag{108}$$

$$F_{i+1/2-} = \mathcal{F}(X_i, X_{i+1}, z_{b,i}, z_{b,i+1}) + \mathcal{S}_{i+1/2-}. \tag{109}$$

$\mathcal{F}$ is a numerical flux for the conservative part of the system, $\mathcal{S}$ is a convenient discretization of the topography source term.

Since the first two lines of (99) correspond to the classical Saint-Venant system, the numerical fluxes

$$F_{i+1/2\pm} = \begin{pmatrix} F_{h,i+1/2} \\ F_{q_x,i+1/2\pm} \\ F_{q_z,i+1/2} \end{pmatrix}, \tag{110}$$

can be constructed using any numerical solver for the Saint-Venant system. More precisely for $F_{h,i+1/2}$,$F_{q_x,i+1/2\pm}$ we adopt numerical fluxes suitable for the Saint-Venant system with topography [17, 9, 19]. Notice that from the definition (101), since only the second component of $S(X)$ is non zero, only F_{q_x} has two interface values under the form $F_{q_x,i+1/2\pm}$. For the definition of $F_{q_z,i+1/2}$, the formula (see [4])

$$F_{q_z,i+1/2} = F_{h,i+1/2} w_{i+1/2}, \tag{111}$$

with

$$w_{i+1/2} = \begin{cases} w_i & \text{if } F_{h,i+1/2} \geq 0 \\ w_{i+1} & \text{if } F_{h,i+1/2} < 0 \end{cases} \tag{112}$$

can be used. The fluxes $F_{\hat{p},i}$ are defined similarly to (111),(112) but on the staggered grid by the following formula

$$F_{\hat{p},i} = \frac{F_{h,i+1/2} + F_{h,i-1/2}}{2}\hat{p}_i, \tag{113}$$

with

$$\hat{p}_i = \begin{cases} \hat{p}_{i-1/2} & \text{if } \frac{F_{h,i+1/2}+F_{h,i-1/2}}{2} \geq 0 \\ \hat{p}_{i+1/2} & \text{if } \frac{F_{h,i+1/2}+F_{h,i-1/2}}{2} < 0 \end{cases}$$

Combining the finite volume approach for the hyperbolic part with a finite difference strategy for the parabolic part, the non-hydrostatic part R_i is defined by

$$R_i = \begin{pmatrix} 0 \\ \nabla^{\gamma}_{sw,i}\, p \end{pmatrix},$$

where the two components of $\nabla^{\gamma}_{sw,i}\, p$ are defined (see (102)) by

$$\Delta x_i \left.\nabla^{\gamma}_{sw,i} p\right|_1 = h_i(p_{i+1/2} - p_{i-1/2}) + \frac{p_{i+1/2}}{2}(\zeta_{i+1} - \zeta_i) + \frac{p_{i-1/2}}{2}(\zeta_i - \zeta_{i-1}), \tag{114}$$

$$\Delta x_i \left.\nabla^{\gamma}_{sw,i} p\right|_2 = -\frac{\gamma}{2}\Big(\Delta x_{i+1/2} p_{i+1/2} + \Delta x_{i-1/2} p_{i-1/2}\Big), \tag{115}$$

with $\zeta_i = h_i + \frac{\gamma^2}{2} z_{b,i}$. And in (107), $\mathrm{div}^{\gamma}_{sw,i+1/2}(\mathbf{u})$ is defined by

$$\begin{aligned}\Delta x_{i+1/2}\mathrm{div}^{\gamma}_{sw,i+1/2}(\mathbf{u}) =& \frac{h_{i+1}+h_i}{2}(u_{i+1}-u_i) - \frac{u_i+u_{i+1}}{2}(z_{b,i+1}-z_{b,i}) \\ &+ \frac{\gamma\Delta x_{i+1/2}}{2}(w_{i+1}+w_i) \\ =& (hu)_{i+1} - (hu)_i - \frac{u_i+u_{i+1}}{2}(\zeta_{i+1}-\zeta_i) \\ &+ \frac{\gamma\Delta x_{i+1/2}}{2}(w_{i+1}+w_i).\end{aligned} \tag{116}$$

Notice that in the definitions (114)-(115) and in the sequel, the quantity p means $\{p_j\}$. Likewise in Eq. (116) and in the sequel, $\mathbf{u}$ means $\{\mathbf{u}_j\}$ for $1 \le j \le I$.

4.3 Stability of the scheme

Using the definitions (104),(105),(106),(107),(114) and (115), the fully discrete scheme for the system (99)-(100) writes

$$\begin{cases} X_i^{n+1/2} = X_i^n - \frac{\Delta t^n}{\Delta x_i}\left(F^n_{i+1/2-} - F^n_{i-1/2+}\right), \\ (h\hat{p})^{n+1/2}_{i+1/2} = (h\hat{p})^n_{i+1/2} - \frac{\Delta t^n}{\Delta x_{i+1/2}}\left(F^n_{\hat{p},i+1} - F^n_{\hat{p},i}\right), \end{cases} \tag{117}$$

$$\begin{cases} p^{n+1/2,k+1}_{i+1/2} = p^{n+1/2,k}_{i+1/2} - \frac{\Delta t^n}{\varepsilon K h^{n+1}}\mathrm{div}^{\gamma}_{sw,i+1/2}\,\mathbf{u}^{n+1/2,k}, \\ \mathbf{u}_i^{n+1/2,k+1} = \mathbf{u}_i^{n+1/2,k} - \frac{\Delta t^n}{K h^{n+1}}\nabla^{\gamma}_{sw,i}\,p^{n+1/2,k+1}. \end{cases} \tag{118}$$

The first equation of (104) gives a finite volume scheme for the Saint-Venant system. The choice of numerical fluxes $F_{i+1/2\pm}$ (see [9]) coupled with a numerical treatment of the topography source term e.g. using the hydrostatic reconstruction [2] gives a numerical resolution of the Saint-Venant system endowed with strong stability properties [3] that are recalled in Propositions 4 and 5.

Now we focus on the stability condition for the resolution of (105) or equivalently (89). Using the definitions (114) and (115), we obtain the discrete version of the operator

$$\Delta^{\gamma}_{sw} p = \mathrm{div}^{\gamma}_{sw}\left(\frac{1}{h}\nabla^{\gamma}_{sw}\, p\right),$$

with $D_{i+1/2}p = -\Delta x_{i+1/2}\Delta^{\gamma}_{sw,i+1/2}p$ and

$$
\begin{aligned}
D_{i+1/2}p = &- \frac{h_{i+1}}{\Delta x_{i+1}}\Big(p_{i+3/2} - p_{i+1/2}\Big) + \frac{h_i}{\Delta x_i}\Big(p_{i+1/2} - p_{i-1/2}\Big) \\
&- \frac{p_{i+3/2}}{2\Delta x_{i+1}}\Big(\zeta_{i+2} - 2\zeta_{i+1} + \zeta_i\Big) - \frac{\Delta x_i - \Delta x_{i+1}}{\Delta x_{i+1}\Delta x_i} p_{i+1/2}\Big(\zeta_{i+1} - \zeta_i\Big) \\
&- \frac{p_{i-1/2}}{2\Delta x_i}\Big(\zeta_{i+1} - 2\zeta_i + \zeta_{i-1}\Big) \\
&+ \frac{p_{i+3/2}}{4h_{i+1}\Delta x_{i+1}}\Big(\zeta_{i+2} - \zeta_{i+1}\Big)\Big(\zeta_{i+1} - \zeta_i\Big) \\
&+ \frac{p_{i+1/2}}{4}\left(\frac{1}{h_{i+1}\Delta x_{i+1}} + \frac{1}{h_i\Delta x_i}\right)\Big(\zeta_{i+1} - \zeta_i\Big)^2 \\
&+ \frac{p_{i-1/2}}{4h_i\Delta x_i}\Big(\zeta_{i+1} - \zeta_i\Big)\Big(\zeta_i - \zeta_{i-1}\Big) \\
&+ \frac{\gamma^2\Delta x_{i+1/2}}{4}\Big(\frac{\Delta x_{i+3/2}p_{i+3/2} + \Delta x_{i+1/2}p_{i+1/2}}{\Delta x_{i+1}h_{i+1}} \\
&+ \frac{\Delta x_{i+1/2}p_{i+1/2} + \Delta x_{i-1/2}p_{i-1/2}}{\Delta x_i h_i}\Big). \qquad (119)
\end{aligned}
$$

Using the expression (119), we are now able to precise the CFL type stability condition for the discretized version of Eq. (89) that writes

$$
\begin{aligned}
2 - \frac{(\Delta t^n)^2}{\varepsilon K^2 h_{i+1/2}\Delta x_{i+1/2}}&\left(\frac{h_{i+1}}{\Delta x_{i+1}} + \frac{h_i}{\Delta x_i} + \frac{1}{4}\left(\frac{1}{h_{i+1}\Delta x_{i+1}} + \frac{1}{h_i\Delta x_i}\right)\Big(\zeta_{i+1} - \zeta_i\Big)^2\right. \\
&\left. - \frac{\Delta x_i - \Delta x_{i+1}}{\Delta x_{i+1}\Delta x_i}\Big(\zeta_{i+1} - \zeta_i\Big) + \frac{\gamma^2\Delta x_{i+1/2}^2}{4}\left(\frac{1}{h_{i+1}\Delta x_{i+1}} + \frac{1}{h_i\Delta x_i}\right)\right) \geq 0,
\end{aligned}
$$

that is fulfilled for

$$
\begin{aligned}
K^2 \geq \frac{(\Delta t^n)^2}{2\varepsilon h_{i+1/2}\Delta x_{i+1/2}}&\left(\frac{h_{i+1}}{\Delta x_{i+1}} + \frac{h_i}{\Delta x_i} + \frac{1}{4}\left(\frac{1}{h_{i+1}\Delta x_{i+1}} + \frac{1}{h_i\Delta x_i}\right)\Big(\zeta_{i+1} - \zeta_i\Big)^2\right. \\
&\left. + \frac{|\Delta x_i - \Delta x_{i+1}|}{\Delta x_{i+1}\Delta x_i}|\zeta_{i+1} - \zeta_i| + \frac{\gamma\Delta x_{i+1/2}^2}{4}\left(\frac{1}{h_{i+1}\Delta x_{i+1}} + \frac{1}{h_i\Delta x_i}\right)\right). \qquad (120)
\end{aligned}
$$

And the condition (120) is satisfied when

$$
K^2 \geq \frac{(\Delta t^n)^2}{2\varepsilon h_{min}\Delta x_{min}^2}\left(2h_{max} + \frac{2}{h_{min}}(\delta\zeta)_{max}^2 + (\delta\zeta)_{max} + \frac{\gamma^2\Delta x_{max}^2}{2h_{min}}\right),
$$

with $r_{min} = \min_{1\leq i\leq I} r_i$, $r_{max} = \max_{1\leq i\leq I} r_i$ for $r = h, \Delta x, \delta\zeta$.

The fully discrete scheme (117),(118) satisfies the following stability properties.

Proposition 4 *Assuming a suitable CFL condition associated with the chosen numerical fluxes* (110) *for the hyperbolic part, the scheme obtained coupling the semi-discretizations* (104),(105) *and* (106),(107)

(i) preserves the nonnegativity of the water depth i.e. $h_i^n \geq 0$, $\forall i$, $\forall n$,
(ii)preserves the steady state of the lake at rest,
(iii)is consistent with the model (99)-(100).

Let us consider that, under a suitable CFL condition associated with the time discretization (104) and the chosen numerical fluxes $F_{h,i\pm1/2}$ and $F_{q_x,i\pm1/2}$ in (110), the numerical approximation of the Saint-Venant part of Eq. (99) allows to obtain a discrete entropy inequality under the form

$$\Delta x_i (E_i^{sv})^{n+1/2} = \Delta x_i (E_i^{sv})^n - \Delta t^n \left(\mathcal{G}_{i+1/2}^n - \mathcal{G}_{i-1/2}^n \right) + \mathcal{D}_i^n, \tag{121}$$

with $E_i^{sv} = \frac{h_i}{2} u_i^2 + \frac{g}{2}(\eta_i^2 - z_{b,i}^2)$ and where $\mathcal{G}_{i\pm1/2}^n$ are numerical fluxes. $\mathcal{D}_i^n$ is a nonpositive term and contains typically two different contributions: the numerical dissipation coming from the upwinding in the space discretization and the error due to the explicit time scheme.

Then assuming (121), we now prove that the numerical scheme (117),(118) satisfies a discrete entropy inequality.

Proposition 5 *The scheme* (104),(105),(106),(107) *satisfies the following entropy inequality*

$$\Delta x_i \bar{E}_i^{n+1} = \Delta x_i \bar{E}_i^n - \Delta t^n \left(\bar{\mathcal{G}}_{i+1/2}^n - \bar{\mathcal{G}}_{i-1/2}^n \right) + \bar{\mathcal{D}}_i^n, \tag{122}$$

with $\bar{E}_i = E_i^{sv} + \frac{h_i}{2} w_i^2 + \frac{\varepsilon}{2} h_i \widetilde{p_i^2}$ *and*

$$\bar{\mathcal{G}}^n_{i+1/2} = \mathcal{G}^n_{i+1/2} + F^n_{h,i+1/2}\frac{(w^n_{i+1/2})^2}{2} + \varepsilon F^n_{h,i+1}\frac{(\hat{p}^n_{i+1})^2}{2} + \frac{1}{2K}\sum_{k=1}^{K}(h^{n+1}_{i+1}u^{n+1/2,k}_{i+1}p^{n+1/2,k+1}_{i+1}),$$

$$\Delta x_i(\widetilde{h_i\hat{p}_i^2})^{n+1} = \frac{1}{2K}\sum_{k=1}^{K}\left(\Delta x_{i+1/2}\frac{h^{n+1}_{i+1/2}}{2}\left(\hat{p}^{n+1/2,k+1}_{i+1/2}\right)^2 + \Delta x_{i-1/2}\frac{h^{n+1}_{i-1/2}}{2}\left(\hat{p}^{n+1/2,k+1}_{i-1/2}\right)^2\right),$$

$$\begin{aligned}
\Delta x_i\bar{\mathcal{D}}^n_i = {} & \Delta x_i\mathcal{D}^n_i + \Delta t^n\left(\left[F^n_{h,i+1/2}\right]_-(w^n_{i+1}-w^n_i)^2 - \left[F^n_{h,i-1/2}\right]_+(w^n_i-w^n_{i-1})^2\right)\\
& + \frac{\Delta t^n}{2}\left(\frac{F^n_{h,i+1}}{2}(\hat{p}^n_{i+1}-\hat{p}^n_{i+1/2})^2 - \frac{F^n_{h,i}}{2}(\hat{p}^n_i-\hat{p}^n_{i+1/2})^2\right)\\
& + \frac{\Delta t^n}{2}\left(\frac{F^n_{h,i}}{2}(\hat{p}^n_i-\hat{p}^n_{i-1/2})^2 - \frac{F^n_{h,i-1}}{2}(\hat{p}^n_{i-1}-\hat{p}^n_{i-1/2})^2\right)\\
& + \frac{\Delta x_i h^{n+1}_i}{2}(w^{n+1/2}_i - w^n_i)^2 + \frac{\Delta x_{i+1/2}h^{n+1}_{i+1/2}}{2}(\hat{p}^{n+1/2}_{i+1/2}-\hat{p}^n_{i+1/2})^2\\
& + \frac{\Delta x_{i-1/2}h^{n+1}_{i-1/2}}{2}(\hat{p}^{n+1/2}_{i-1/2}-\hat{p}^n_{i-1/2})^2\\
& - \sum_{k=1}^{K}\frac{\Delta x_{i+1/2}h^{n+1}_{i+1/2}}{2}\left(\varepsilon\left(\hat{p}^{n+1/2,k+1}_{i+1/2}-\hat{p}^{n+1/2,k}_{i+1/2}\right)^2 - \left|\mathbf{u}^{n+1/2,k+1}_{i+1/2}-\mathbf{u}^{n+1/2,k}_{i+1/2}\right|^2\right)\\
& - \sum_{k=1}^{K}\frac{\Delta x_{i+1/2}h^{n+1}_{i-1/2}}{2}\left(\varepsilon\left(\hat{p}^{n+1/2,k+1}_{i-1/2}-\hat{p}^{n+1/2,k}_{i-1/2}\right)^2 - \left|\mathbf{u}^{n+1/2,k+1}_{i-1/2}-\mathbf{u}^{n+1/2,k}_{i-1/2}\right|^2\right)\\
& + \mathcal{O}\left(\frac{\Delta x_i}{\varepsilon}\right).
\end{aligned}$$

Equation (122) is a discrete version of (98).

Remark 8 When considering the semi-descrete in space scheme detailed in Section 4.2, a semi-discrete in space version of (122) holds where all the non-negative terms in the expression of $\bar{\mathcal{D}}^n_i$ corresponding to time discretisation errors vanish.

Proof (Proof of prop. 4) *(i)* The statement that $\mathcal{F}$ preserves the nonnegativity of the water depth means exactly that

$$F_h(h_i = 0, u_i, h_{i+1}, u_{i+1}) - F_h(h_{i-1}, u_{i-1}, h_i = 0, u_i) \leq 0,$$

for all choices of the other arguments. From (104),(106),(108) and (109), we need to check that, with obvious notations

$$F_h(X^n_{i+1/2}, X^n_{i+1/2+}) - F_h(X^n_{i-1/2}, X^n_{i-1/2+}) \leq 0,$$

whenever $h^n_i = 0$. And this property holds typically when the hydrostatic reconstruction (HR) is used to approximate the topography source term since for the HR technique $h_i = 0$ implies $h_{i+1/2-} = h_{i-1/2+} = 0$, see [2].

(ii) When $u_i^n = 0$ for all i, the properties of the hydrostatic reconstruction technique ensure $F^n_{i+1/2-} = F^n_{i-1/2+}$ in (104),(106) and $F^n_{p,i+1-} = F^n_{p,i+}$ in (107). Moreover since $u_i^n = 0\ \forall\, i$ we have $R_i = 0$ in (106) and $\mathrm{div}^{\gamma}_{sw,i+1/2}(\{\mathbf{u}\}) = 0$ in (107). Therefore $\forall\, i$

$$X_i^{n+1} = X_i^n, \quad \text{and} \quad p^{n+1}_{i+1/2} = p^n_{i+1/2},$$

proving that the scheme is well-balanced.

(iii) The discretization (104),(105) is an explicit first order time scheme. The numerical fluxes defined by (108),(109) and (113) are a consistent discretization of the hyperbolic part of the system (99),(100) without topography. Likewise, the hydrostatic reconstruction applied to the fluxes (110),(113) gives a consistent discretization of the system (99),(100) with topography and the discretizations (114),(115) being obviously consistent with the dispersive part, this proves the result. □

Proof (Proof of prop. 5) Since we have assumed that the kinetic energy of the Saint-Venant part of Eq. (99) satisfies (121), this means that the first two components of the first equation of (117) multiplied respectively by $gh_i^n - (u_i^n)^2/2$ and u_i^n give Eq. (121). It remains to consider the contributions to the energy balance of the last two components of (117) and of Eq. (118).

First let us multiply the third component of the first equation of (117) by w_i^n, then we get

$$\frac{h_i^{n+1}}{2}(w_i^{n+1/2})^2 - \frac{h_i^n}{2}(w_i^n)^2 + \frac{\Delta t^n}{\Delta x_i}\left(F^n_{h,i+1/2}\frac{(w^n_{i+1/2})^2}{2} - F^n_{h,i-1/2}\frac{(w^n_{i-1/2})^2}{2}\right) =$$

$$\frac{\Delta t^n}{\Delta x_i}\left(\left[F^n_{h,i+1/2}\right]_-(w^n_{i+1} - w^n_i)^2 - \left[F^n_{h,i-1/2}\right]_+(w^n_i - w^n_{i-1})^2\right) + \frac{h_i^{n+1}}{2}(w_i^{n+1/2} - w_i^n)^2,$$

with the notations $[a]_+ = max(a,0)$, $[a]_- = min(a,0)$ $a = [a]_+ + [a]_-$ and $w^n_{i+1/2}$ is defined by (112). Then we multiply the last component of Eq. (117) by $p^n_{i+1/2} + \frac{g}{2}h^n_{i+1/2}$ leading to

$$\begin{aligned}\frac{h^{n+1}_{i+1/2}}{2}\left(\hat{p}^{n+1/2}_{i+1/2}\right)^2 - \frac{h^n_{i+1/2}}{2}\left(\hat{p}^n_{i+1/2}\right)^2 + \frac{\Delta t^n}{\Delta x_{i+1/2}}\left(F^n_{h,i+1}\frac{(\hat{p}^n_{i+1})^2}{2} - F^n_{h,i}\frac{(\hat{p}^n_i)^2}{2}\right)\\ = \frac{\Delta t^n}{\Delta x_{i+1/2}}\left(\frac{F^n_{h,i+1}}{2}(\hat{p}^n_{i+1} - \hat{p}^n_{i+1/2})^2 - \frac{F^n_{h,i}}{2}(\hat{p}^n_i - \hat{p}^n_{i+1/2})^2\right)\\ + \frac{h^{n+1}_{i+1/2}}{2}\left(\hat{p}^{n+1/2}_{i+1/2} - \hat{p}^n_{i+1/2}\right)^2,\end{aligned}$$

with $F_{h,i+1} = (F_{h,i+3/2} + F_{h,i+1/2})/2$. Thanks to the definition (4.2), the two quantities

$$\frac{F^n_{h,i+1}}{2}(\hat{p}^n_{i+1} - \hat{p}^n_{i+1/2})^2, \quad \text{and} \quad -\frac{F^n_{h,i}}{2}(\hat{p}^n_i - \hat{p}^n_{i-1/2})^2,$$

are always non-positive.

Second, we multiply the equations (118) respectively by $\hat{p}_{i+1/2}^{n+1/2,k+1}$ and $\mathbf{u}_i^{n+1/2,k}$ and sum the obtained relations for $k = 1, \dots K$. Since the definitions (114),(115) ensure a discrete version of the duality relation (103) under the form

$$\begin{aligned}\frac{\nabla_{sw,i}^{\gamma} p^{n+1/2,k+1}}{\Delta x_i} \cdot \mathbf{u}_i^{n+1/2,k} &= e_{i+1/2}^{n+1/2,k+1/2} - e_{i-1/2}^{n+1/2,k+1/2} \\ &- \frac{1}{2\Delta x_{i+1/2}} \mathrm{div}_{sw,i+1/2}^{\gamma}(\mathbf{u}^{n+1/2,k}) p_{i+1/2}^{n+1/2,k+1} \\ &- \frac{1}{2\Delta x_{i-1/2}} \mathrm{div}_{sw,i-1/2}^{\gamma}(\mathbf{u}^{n+1/2,k}) p_{i-1/2}^{n+1/2,k+1}, \end{aligned} \tag{123}$$

with

$$e_{i+1/2}^{n+1/2,k+1/2} = \frac{1}{2}\Big(h_{i+1}^{n+1} u_{i+1}^{n+1/2,k} p_{i+1/2}^{n+1/2,k+1} - h_i^{n+1} u_i^{n+1/2,k} p_i^{n+1/2,k+1}\Big).$$

The duality relation (123) has been written for the variable $p_{i\pm1/2}^{n+1/2,k+1}$ but the last two terms in (123) should be a discrete version of the r.h.s. of Eq. (57) i.e. of the quantity $\hat{p}\mathrm{div}_{sw}^{\gamma}(\mathbf{u})$. And since $\hat{p} = p + gh/2$ the reminder is

$$\frac{g}{2} h_{i+1/2}^{n+1} \mathrm{div}_{sw,i+1/2}^{\gamma}(\mathbf{u}^{n+1/2,k}) = O\left(\frac{\Delta x_{i+1/2}}{\varepsilon}\right),$$

giving the expressions of the terms denoted $h_i^{n+1}\hat{w}_i^{n+1/2}$ and $h_i^{n+1}(\hat{u}_i^{n+1/2})^2$ and given in (122).

For the errors coming from the time dicretization of Eqs. (118), we have

$$\begin{aligned}\Big((hp)_{i+1/2}^{n+1/2,k+1} - (hp)_{i+1/2}^{n+1/2,k}\Big)\hat{p}_{i+1/2}^{n+1/2,k+1} &= \Big((h\hat{p})_{i+1/2}^{n+1/2,k+1} - (h\hat{p})_{i+1/2}^{n+1/2,k}\Big)\hat{p}_{i+1/2}^{n+1/2,k+1} \\ &= \frac{1}{2}(h\hat{p}^2)_{i+1/2}^{n+1/2,k+1} - \frac{1}{2}(h\hat{p}^2)_{i+1/2}^{n+1/2,k} \\ &\quad + \frac{h_{i+1/2}^{n+1}}{2}\Big(\hat{p}_{i+1/2}^{n+1/2,k+1} - \hat{p}_{i+1/2}^{n+1/2,k}\Big)^2, \\ \Big((h\mathbf{u})_i^{n+1/2,k+1} - (h\mathbf{u})_i^{n+1/2,k}\Big) \cdot \mathbf{u}_i^{n+1/2,k} &= \frac{h_i^{n+1}}{2}|\mathbf{u}_i^{n+1/2,k+1}|^2 - \frac{h_i^{n+1}}{2}|\mathbf{u}_i^{n+1/2,k}|^2 \\ &\quad - \frac{h_{i+1/2}^{n+1}}{2}\Big|\mathbf{u}_{i+1/2}^{n+1/2,k+1} - \mathbf{u}_{i+1/2}^{n+1/2,k}\Big|^2. \end{aligned}$$

Summing the previous relations for $k = 1, \dots, K$ and adding the result to the other contributions gives the corresponding expressions appearing in relation (122). This ends the proof. □

4.4 Higher order schemes

Basically, for the discretization of the model (93)-(96), we have presented a first order scheme in space and time. Second order extensions (in space and time) can be proposed see [1].

4.5 Simulation results

In this paragraph, only few numerical examples are presented. A more complete validation of the numerical procedure will be presented in a companion paper. Notice that in the 1d case, we mainly validate the numerical scheme but the reduction of the computation costs will be more significant in a two-dimensional setting.

4.5.1 Dingemans experiments

The experiments carried out by Dingemans [13] at Delft Hydraulics deal with the wave propagation over uneven bottoms. A small amplitude wave (0.02 m) is generated at the left boundary of a closed basin with vertical shores. At rest, the water depth in the channel varies from 0.4 m to 0.1 m, see Fig. 3. Eight sensors recording the free surface elevation are located at abscissa 2 m, 4 m, 10.5 m, 12.5 m, 13.5 m, 14.5 m, 15.7 m and 17.3 m.

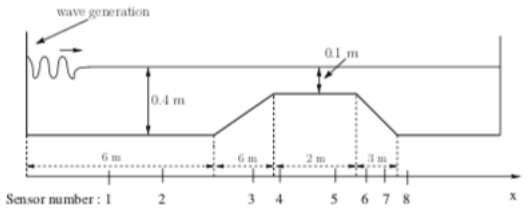

Fig. 3 Channel profile for the experiments and location of the sensors.

For $\gamma = \sqrt{3}$, we compare the simulations results obtained with the two numerical schemes (the one proposed in [1] and the one proposed in this paper with $\varepsilon = 1/c^2 = 10^{-4}$ m^{-2}.s^2). The results obtained with a uniform mesh of 1600 nodes are depicted over Fig. 4 where the computed and measured free surface elevations at four points are presented. Notice that for $\varepsilon = 10^{-7}$ m^{-2}.s^2, the simulations of the complete and relaxed model cannot be distinguished.

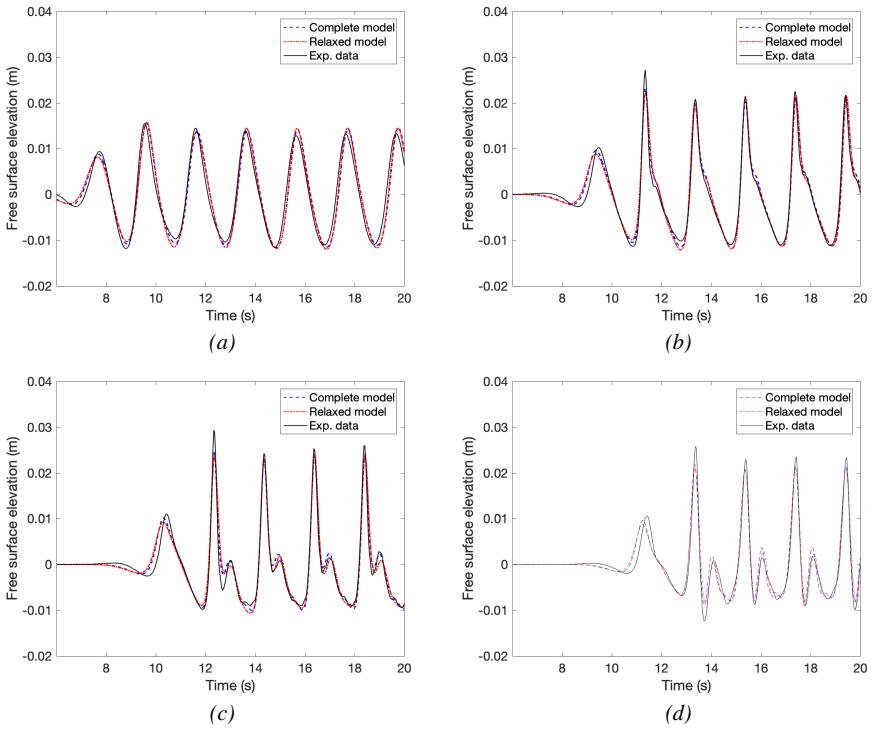

Fig. 4 Comparisons between the experimental data (solid line) and the simulations of the dispersive model with the model presented in [1] (blue dashed line) and with the relaxed model presented in this paper (red dashed-dotted line). Figs. *(a)*, *(b)*, *(c)* and *(d)* respectively correspond to the results for the sensors 3, 4, 5 and 6.

4.5.2 Comparison of the computational costs

For the simulation results given in paragraph 4.5.1, we compare the computational costs of the numerical schemes with and without pseudo-compressibility effects. More precisely, we compare the CPU time necessary to simulate the test case presented in paragraph 4.5.1 with the method proposed in [1] – corresponding to an incompressible model and requiring to solve the elliptic equation (88) – and the proposed explicit in time scheme (83)-(84) with the pseudo-compressible effects.

The advantages of the model and numerical srategy presented in this paper are significant for 2d problems with a large number of nodes but can hardly be highlighted in the 1d case where the elliptic operator to inverse is a symmetric tridagonal matrix. Hence, in order to illustrate the interest of the proposed scheme, we have used a conjugate gradient technique mimicking what would be done to solve (88) in 2d for an unstructured mesh.

Figure 5 presents the CPU time required to perform the simulations of the Dinguemans experiment with several meshes namely with 2000, 4000, 8000, 16000 and 32000 nodes. It appears that when the number of nodes increases, the proposed explicit in time scheme is more efficient than the conjugate gradient algorithm (used here without preconditioning). Notice that the authors have not performed an exhaustive comparison between the costs of the conjugate gradient technique – for which several optimizations are possible – and the iterative and explicit time resolution scheme (83)-(84).

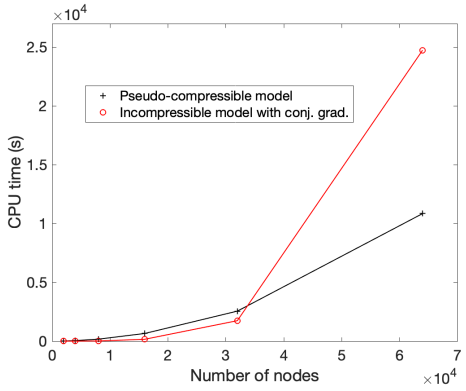

Fig. 5 Computational costs necessary to simulate the Dinguemans experiment with several meshes.

4.5.3 The acoustic waves

For the test case depicted in paragraph 4.5.1, the basin is at rest at the initial instant and we give at time $t = 0.01$ s, the value of the quantity $\varepsilon(p + gh/2)$ representing the pseudo-compressible effects. It appears over Fig. 6 that at time $t = 0.1$ s, whereas the free surface has just begun to deform at the boundary where the wave is generated, the acoustic-type waves have already propagated in the basin.

Acknowledgements

The authors thank FranÃğois Bouchut for his helpful and constructive discussions that greatly contributed to improve the final version of the paper.

References

1. N. Aïssiouene, M.-O. Bristeau, E. Godlewski, A. Mangeney, C. Parés, and J. Sainte-Marie, *A two-dimensional method for a family of dispersive shallow water model*, working paper or preprint, May 2019.

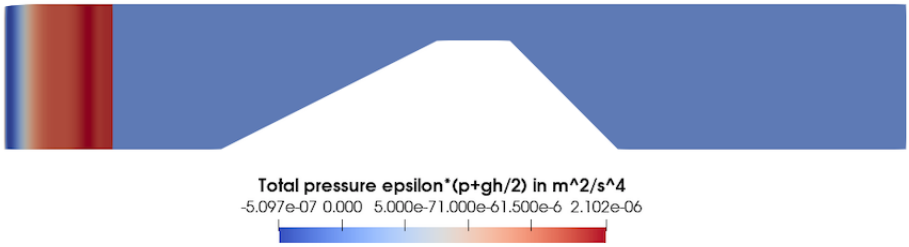

Fig. 6 Variations of the quantity $x \mapsto \varepsilon(p + gh/2)$ with $\varepsilon = 10^{-7}$ m^{-2}.s^2 at time $t = 0.01$ s.

2. E. Audusse, F. Bouchut, M.-O. Bristeau, R. Klein, and B. Perthame, *A fast and stable well-balanced scheme with hydrostatic reconstruction for Shallow Water flows*, SIAM J. Sci. Comput. **25** (2004), no. 6, 2050–2065.
3. E. Audusse, F. Bouchut, M.-O. Bristeau, and J. Sainte-Marie, *Kinetic entropy inequality and hydrostatic reconstruction scheme for the Saint-Venant system*, Math. Comp. **85** (2016), no. 302, 2815–2837. MR 3522971
4. E. Audusse and M.-O. Bristeau, *Transport of pollutant in shallow water flows : A two time steps kinetic method*, ESAIM: M2AN **37** (2003), no. 2, 389–416.
5. ———, *A well-balanced positivity preserving second-order scheme for Shallow Water flows on unstructured meshes*, J. Comput. Phys. **206** (2005), no. 1, 311–333.
6. A.-J.-C. Barré de Saint-Venant, *Théorie du mouvement non permanent des eaux avec applications aux crues des rivières et à l'introduction des marées dans leur lit*, C. R. Acad. Sci. Paris **73** (1871), 147–154.
7. J.-L. Bona, T.-B. Benjamin, and J.-J. Mahony, *Model equations for long waves in nonlinear dispersive systems*, Philos. Trans. Royal Soc. London Series A **272** (1972), 47–78.
8. J.L. Bona, M. Chen, and J.-C. Saut, *Boussinesq equations and other systems for small-amplitude long waves in nonlinear dispersive media: Part I. Derivation and linear theory*, J. Nonlinear Sci. **12** (2002), 283–318.
9. F. Bouchut, *Nonlinear stability of finite volume methods for hyperbolic conservation laws and well-balanced schemes for sources*, Birkhäuser, 2004.
10. M.-O. Bristeau, A. Mangeney, J. Sainte-Marie, and N. Seguin, *An energy-consistent depth-averaged euler system: Derivation and properties*, Discrete and Continuous Dynamical Systems - Series B **20** (2015), no. 4, 961–988.
11. R. Camassa, D. D. Holm, and C. D. Levermore, *Long-time effects of bottom topography in shallow water*, Phys. D **98** (1996), no. 2-4, 258–286, Nonlinear phenomena in ocean dynamics (Los Alamos, NM, 1995). MR 1422281 (98a:76005)
12. A. J. Chorin, *Numerical solution of the Navier-Stokes equations*, Math. Comp. **22** (1968), 745–762. MR 0242392 (39 #3723)
13. M.-W. Dingemans, *Wave propagation over uneven bottoms*, Advanced Series on Ocean Engineering - World Scientific, 1997.
14. V. Duchêne, *Rigorous justification of the Favrie-Gavrilyuk approximation to the Serre-Green-Naghdi model*, Nonlinearity **32** (2019), no. 10, 3772–3797.
15. R. Fine and F. Millero, *Compressibility of Water as a Function of Temperature and Pressure*, The Journal of Chemical Physics **59** (1973), no. 10, 5529–5536.
16. J.-F. Gerbeau and B. Perthame, *Derivation of Viscous Saint-Venant System for Laminar Shallow Water; Numerical Validation*, Discrete Contin. Dyn. Syst. Ser. B **1** (2001), no. 1, 89–102.
17. E. Godlewski and P.-A. Raviart, *Numerical approximation of hyperbolic systems of conservation laws*, Applied Mathematical Sciences, vol. 118, Springer, New York, 1996.

18. A.E. Green and P.M. Naghdi, *A derivation of equations for wave propagation in water of variable depth*, J. Fluid Mech. **78** (1976), 237–246.
19. R.-J. LeVeque, *Finite volume methods for hyperbolic problems*, Cambridge University Press, 2002.
20. O. Nwogu, *Alternative form of Boussinesq equations for nearshore wave propagation*, Journal of Waterway, Port, Coastal and Ocean Engineering, ASCE **119** (1993), no. 6, 618–638.
21. D.H. Peregrine, *Long waves on a beach*, J. Fluid Mech. **27** (1967), 815–827.